Published OnlineFirst February 23, 2011; DOI:10.1158/1078-0432.CCR-10-2008



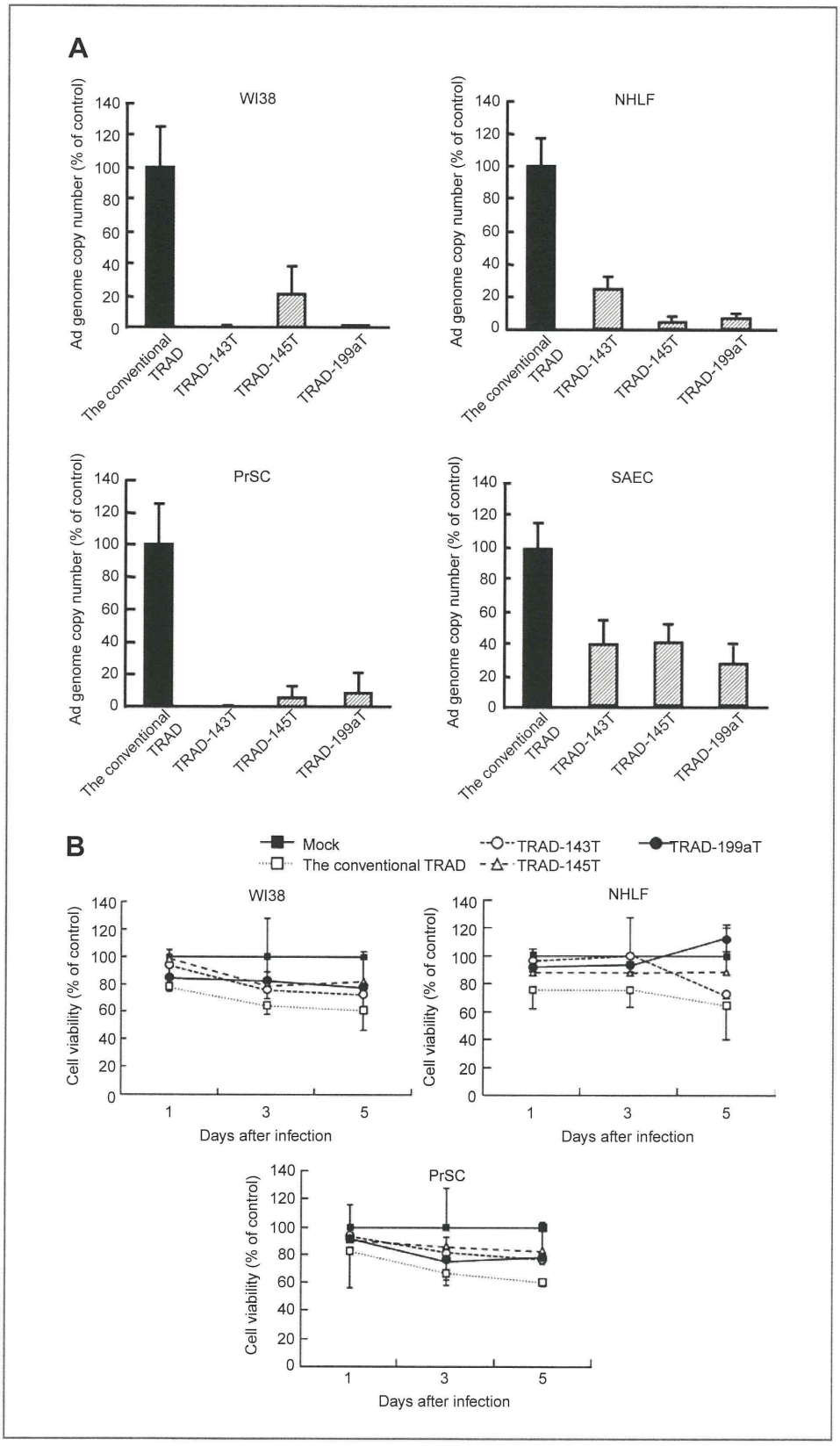


Figure 4. Reduced replication of TRADs in normal human cells by insertion of the miRNA complementary sequences. A, the viral genome copy numbers of TRADs in normal cells. The cells were infected with the TRADs at an MOI of 10 for 2 hours. Five days after infection, the viral genome copy numbers were determined by real-time PCR. B, time-course study of the normal human cell viabilities after infection with TRADs by Alamar blue assay. The cells were infected with the TRADs at an MOI of 10 for 2 hours. At the indicated time points, the viability of the cells was analyzed by Alamar blue assay. The data were normalized by the data of the mock-infected group. C, restoration of TRAD replication in human normal cells by 2′-*O*-methylated antisense oligonucleotides. The cells were transfected with 50 nmol/L of 2′-*O*-methylated antisense oligonucleotides for miR-143 or -199a. Twenty-four hours after transfection, the cells were infected with the TRADs at an MOI of 10, and the viral genome copy numbers were determined 5 days after infection with the TRADs. D, the E1A mRNA levels in normal human cells. The cells were infected with the TRADs at an MOI of 10 for 1.5 hours. Twenty-four hours after infection, the E1 mRNA levels were determined by real-time RT-PCR. The data was normalized by the data of the conventional TRAD group. All the data are shown as the means ± SD ($n = 3$–4). *, $P < 0.05$; **, $P < 0.005$.

Published OnlineFirst February 23, 2011; DOI:10.1158/1078-0432.CCR-10-2008



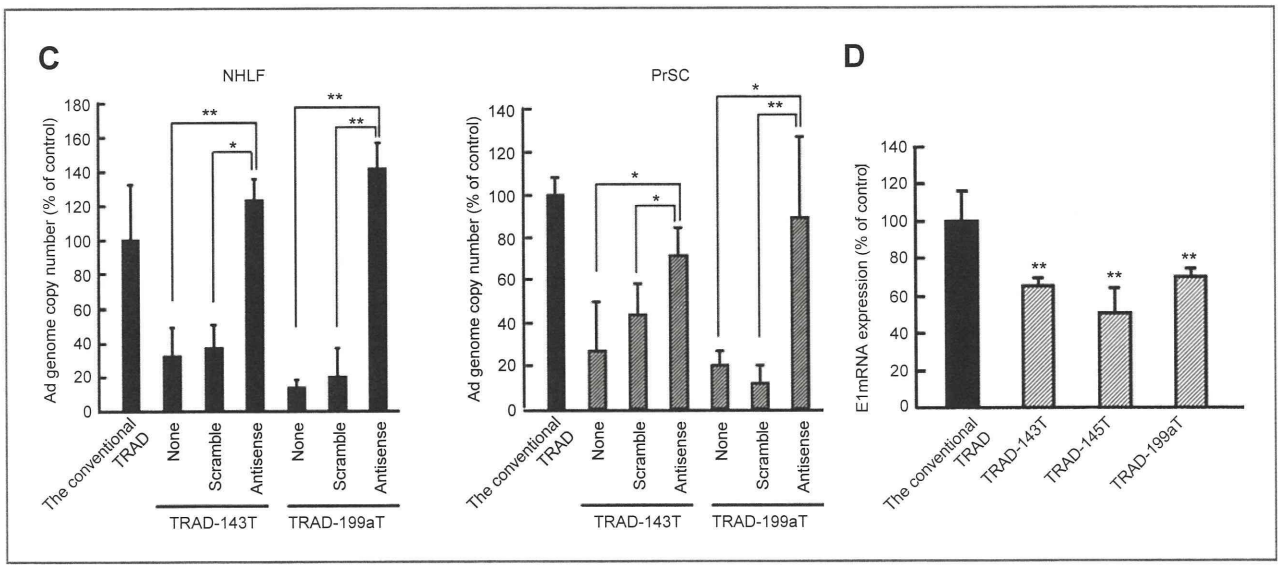


Figure 4. (*Continued*)

### *E1A* expression by TRAD-miRT in normal cells

To determine whether incorporation of the miRNA complementary sequences into the *E1* gene expression cassette decreases the *E1* mRNA levels in normal human cells, real-time RT-PCR analysis for the E1A mRNA levels wascarried out. The E1A mRNA levels were reduced by more than 30% for TRAD-143T, -145T, and -199aT, compared with the parent TRAD, in NHLF (Fig. 4D). The reduction in the E1A mRNA levels corresponded to the suppression in replication of TRAD-miRT, indicating that miRNA-mediated reduction in the *E1* gene expression resulted in a reduced replication of TRAD-miRT.

### Development of TRADs containing the complementary sequences for liver-specific miRNA

To prevent the replication of TRADs in liver hepatocytes as well as other normal cells, we incorporated not only miR-199a complementary sequences but also sequences complementary to liver-specific miR-122a into the *E1* gene expression cassette, resulting in TRAD-122a/199aT (Fig. 5A). It is well known that Ads have high hepatic tropism, leading to efficient liver accumulation even after local administration. MiR-122a was expressed approximately 100- and 20-fold more abundantly in NHep and Huh-7 cells, respectively, than in the other normal human cells and tumor cells (Fig. 5B); conversely, the other normal cells expressed more than 10-fold lower levels of miR-122a than miR-143, -145, and -199a (data not shown). Incorporation of miR-122a complementary sequences alone significantly reduced the virus genome copy number of TRAD-122aT in NHLF and NHep; however, no statistically significant decrease in the genome copy number of TRAD-122aT was found in PrSC (Fig. 5C). On the other hand, insertion of miR-199a target sequences alone was less efficient than insertion of miR-122a target sequences in NHep, probably due to the lower expression of miR-199a than miR-122a in NHep. By contrast, insertion of both miR-122a and miR-199a target sequences into the *E1* gene expression cassette efficiently reduced the replication of TRAD-122a/199aT by 10- to 50-fold in all normal cells examined. Significantly reduced replication of TRAD-122a and TRAD-122a/199aT was also found in Huh-7 cells, which are a hepatoma cell line highly expressing miR-122a and are often used as a model of hepatocytes (Supplementary Fig. S2). The incorporation of the miR-145 complementary sequences was also effective for suppressing the TRAD replication in NHep (Supplementary Fig. S3). The E1A mRNA levels were reduced for TRAD-122aT and -122a/199aT in NHep (Fig. 5D). In addition, TRAD-122a/199aT efficiently replicated in the tumor cells, resulting in efficient tumor cell lysis (Fig. 5E and F). These results indicate that replication of the TRADs in various types of normal human cells, including liver hepatocytes, is significantly reduced by insertion of the multiple target sequences to both miR-122a and -199a, without influencing the tumor cell lysis activity.

## Discussion

The aim of this study was to prevent the replication of TRADs in normal human cells by incorporation of sequences complementary to miRNAs that are selectively downregulated in tumor cells, without altering the tumor cell lysis activity. Currently, there is no appropriate animal model which fully supports the *in vivo* replication of Ads and evaluation of the *in vivo* toxicity caused by oncolytic Ads, and thus it is important to be cautious in regard to oncolytic Ad-induced toxicity. To prevent the *E1* gene expression and replication of oncolytic Ads in normal cells as much as possible, an miRNA-mediated posttranscriptional detargeting system was included in TRADs, in

Published OnlineFirst February 23, 2011; DOI:10.1158/1078-0432.CCR-10-2008



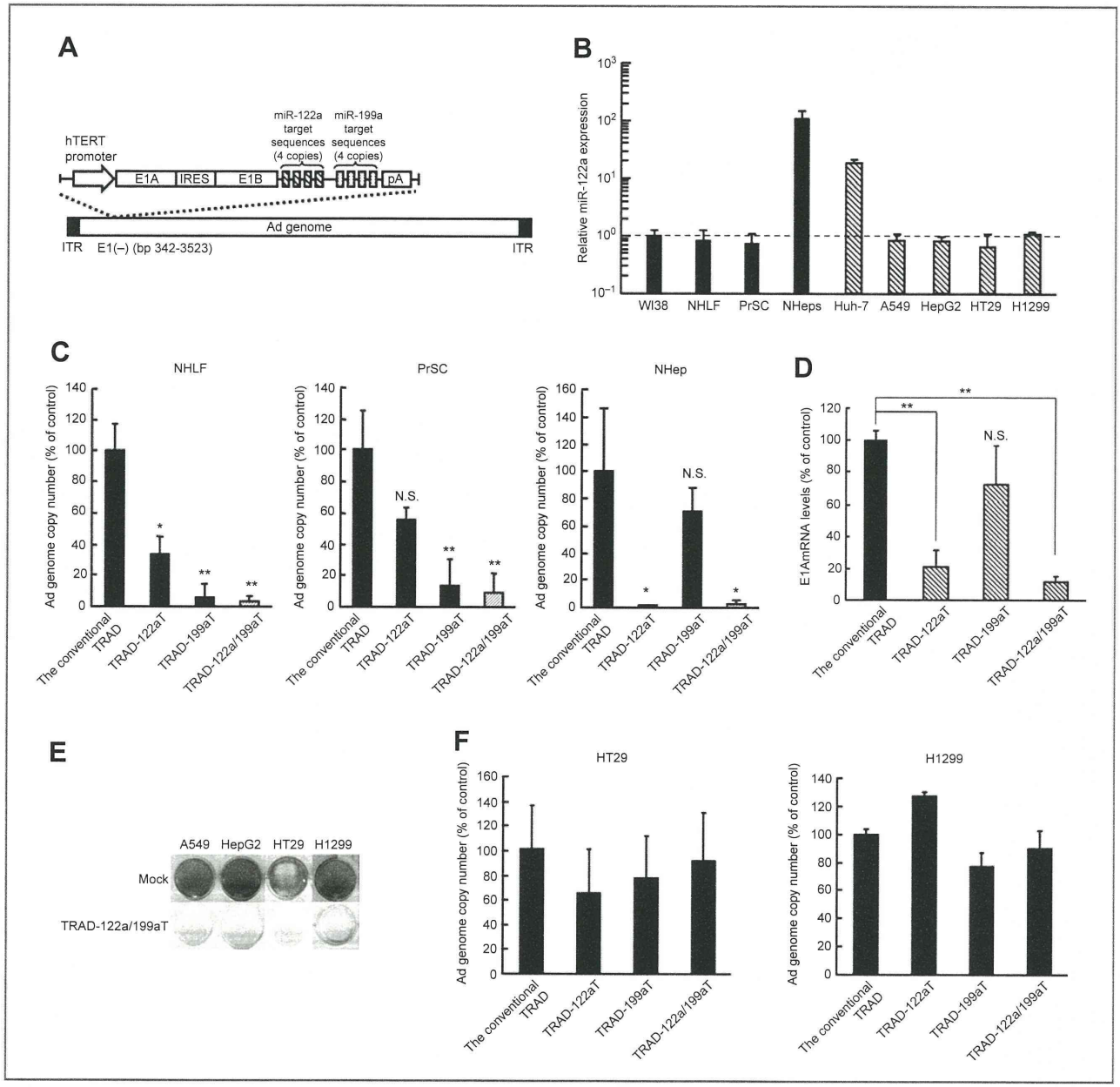


Figure 5. Tumor cell lysis activity and enhanced safety profile of TRAD-122a/199aT. A, a schematic diagram of TRAD-122a/199aT. B, miR-122a expression levels in the normal and tumor cells. C, the viral genome copy numbers of TRAD-122a/199aT in normal human cells. D, the E1A mRNA levels in NHep. E, crystal violet analysis for the cytopathic effects of TRAD-122a/199aT. The results are representative of 2 independent experiments. F, the viral genome copy numbers of TRAD-122a/199aT in tumor cells. The tumor and normal cells were infected with the TRADs at an MOI of 2 (tumor cells) or 10 (normal cells) for 2 hours. The cells were stained with crystal violet 3 days after infection. The viral genome copy numbers were determined 3 (tumor cells) or 5 days (normal cells) after infection. For determination of the E1A mRNA levels, total RNA was isolated from NHep 24 hour after infection with the TRADs at an MOI of 10, and the E1A mRNA levels were determined by real-time RT-PCR. The data was normalized by the data of the conventional TRAD group. All the data are shown as the means ± SD ($n$ = 3–6). N.S.: not significantly different. *, $P < 0.05$; **, $P < 0.005$.

addition to the transcriptional targeting system via tumor-specific promoters.

As described above, TRAD replicates in the injected tumors and is disseminated from the injected tumors into the systemic circulation, leading to infection of distant, uninjected tumors (11, 13, 14). This property of TRAD had led to a concern that TRAD could infect normal cells over the whole body, including the hepatocytes, after dissemination from the injected tumors. It is crucial that such unexpected infection of normal cells by TRAD is prevented. Previous studies have shown that insertion of sequences complementary to liver-specific miR-122a reduced the replication of oncolytic Ads in Huh-7 cells, which are a model cell for hepatocytes (31–33). It is especially crucial

Published OnlineFirst February 23, 2011; DOI:10.1158/1078-0432.CCR-10-2008



to prevent the replication of TRAD in the liver, because Ad vectors have strong hepatotropism. However, TRAD also might infect normal cells other than hepatocytes, indicating that replication of oncolytic Ads in normal cells other than hepatocytes should also be suppressed. To prevent the replication of TRADs in other normal cells, we incorporated the sequences complementary to miR-143, -145, -199a, or let-7a, which are downregulated in the tumors and widely expressed in normal cells. The expression levels of these miRNAs in the tumor cells were lower than those in the normal cells in this study, and insertion of sequences complementary to miR-143, -145, or -199a significantly reduced the E1A mRNA levels and the replication of TRADs in the normal cells.

Overall, among the miRNA complementary sequences, the miR-199a complementary sequences appeared to be the most efficient at suppressing the replication of TRADs across all the normal cells except for hepatocytes; however, insertion of miR-199a target sequences alone failed to significantly reduce the replication of TRADs in the hepatocytes. To simultaneously prevent the replication of TRADs in various types of normal cells, including hepatocytes, we incorporated sequences complementary to miR-122a, which is abundantly expressed in hepatocytes, in addition to miR-199a target sequences. Brown and colleagues reported that a desired transgene expression pattern was achieved, depending on the miRNA expression profile, by incorporation of target sequences for 2 distinct miRNAs (34). TRAD-122aT/199aT exhibited more than 10-fold reduction in the replication in all the normal cells except for SAEC, although insertion of target sequences for miR-122a or miR-199a alone failed to suppress the replication of TRADs in either of the normal cells. Furthermore, TRAD-122aT/199aT and the parental TRAD mediated similar cytopathic efficacies in the tumor cells. These results indicate that replication of TRADs in not only hepatocytes but also other normal cells is simultaneously reduced by insertion of both miR-122a complementary sequences and sequences complementary to miRNAs highly expressed in normal cells, without altering the tumor cell lysis activity.

TRADs containing miR-122a complementary sequences are also considered to be promising for the treatment of liver cancer because miR-122a is significantly downregulated in liver cancer cells (35–37) leading to efficient replication and lytic activity of TRADs containing miR-122a complementary sequences in liver cancer cells. This study has shown that TRAD-122aT/199aT caused efficient cell lysis in a hepatocellular carcinoma cell line, HepG2 cells, while the replication of TRADs containing the miR-122a complementary sequences in normal hepatocytes, which highly express miR-122a, was significantly inhibited.

The expression levels of miRNAs are a crucial factor to suppress the gene expression by miRNAs. Brown and colleagues showed that miRNAs should be expressed at a concentration above the threshold (>100 copies/pg small RNA) to induce miRNA-regulated suppression of transgene expression (34). We were not able to precisely show the expression levels of miRNAs as the ratio of copies/pg small RNA in this study; however, comparing the miRNA levels in this study with those reported by Brown and colleagues (34), we consider that the expression levels of miR-143, -145, and -199a in the normal cells were higher than 100 copies/pg small RNA, leading to efficient suppression of the replication of TRADs.

Several studies have shown that let-7, including let-7a, is significantly downregulated in tumor cells (16, 19, 20). Edge and colleagues reported that insertion of let-7a complementary sequences into the matrix protein expression cassette of the vesicular somatitis virus (VSV) suppressed the replication of VSV in human primary fibroblast MG38 cells; on the other hand, VSV carrying let-7a target sequences efficiently replicated in A549 cells (38). However, our data showed that cancer cell lines other than HepG2 cells expressed similar or higher levels of let-7a than the normal cells. In addition, the expression levels of let-7a were more than 10-fold higher than those of the other miRNAs in the tumor cells. Abundant let-7a expression leads to a reduction in the replication of TRAD-let7aT in tumor cells. Furthermore, the members of the let-7 family, including let-7b and let-7c, have the same seed sequence, suggesting that let-7 family members other than let-7a would also contribute to the significant suppression of replication of TRAD-let7aT. These results suggest that not only expression profiles of miRNAs but also absolute amounts of miRNA expression in the cells are of great importance for miRNA-regulated gene expression.

Our data showed that the E1A mRNA levels were reduced by approximately 30% to 50% for TRAD-143T, -145T, and -199aT, compared with the conventional TRAD 24 hour after infection with the normal cells. These reduction levels in the E1A mRNA were much smaller than those in the Ad genome copy numbers at 5 days after infection; however, these reductions in the E1A mRNA levels would lead to large differences in the Ad genome copy numbers after several virus replication cycles. More than 5-fold reductions in the E1A mRNA were found for TRAD-143T, -145T, and -199aT, compared with the parental TRAD, 5 days after infection with the normal cells (data not shown).

A phase I clinical trial of the parental TRAD was conducted, and serious adverse events were not observed (3). In this study, efficient replication of the conventional TRAD in WI38 cells was found at an MOI of 10; however, the conventional TRAD did not exhibit a high level of replication at an MOI of 2. It might be unlikely that such a high titer (MOI 10) of oncolytic Ad would infect organs distal from the injection points in clinical trials; however, normal cells around the injection points might be infected with a high titer of oncolytic Ad. In addition, even though no apparent replication of TRADs is observed in normal cells after infection of TRADs, the expression of Ad proteins, including E1A and E4 proteins, affects the cellular functions via various mechanisms (39–41). This study indicates that inclusion of an miRNA-regulated *E1* gene expression system in oncolytic Ads enhances the safety of oncolytic Ads and makes it possible to increase the injection doses, leading to superior therapeutic effects.

Published OnlineFirst February 23, 2011; DOI:10.1158/1078-0432.CCR-10-2008



In summary, we developed TRADs in which the *E1* gene expression is controlled by miRNAs more highly expressed in normal cells than tumor cells. The TRADs containing the sequences complementary to miR-143, -145, or -199a exhibited reduced replication in the normal cells without altering the tumor cell lysis activity. Furthermore, incorporation of both miR-199a and miR-122a target sequences significantly suppressed the replication in all human primary cells examined, including hepatocytes. TRAD-miRT has enhanced both the safety profiles and comparable tumor cell lysis activity to the parental TRAD, suggesting that TRAD-miRT offers great potential for the treatment of tumors.

## Disclosure of Potential Conflicts of Interest

Toshiyoshi Fujiwara and Hiroyuki Mizuguchi are consultants to Oncolys BioPharma, Inc. No other potential conflicts of interest were disclosed.

## Acknowledgments

We thank Takako Ichinose, Koyori Yano (National Institute of Biomedical Innovation, Osaka, Japan), and Sayuri Okamoto (Graduate School of Pharmaceutical Sciences, Osaka University, Osaka, Japan) for their help.

## Grant Support

Support was received from a grant-in-aid for Young Scientists (A) F. Sakurai from the Ministry of Education, Culture, Sports, Science, and Technology (MEXT) of Japan (F. Sakurai), and a grant from the Takeda Science Foundation (H. Mizuguchi).

The costs of publication of this article were defrayed in part by the payment of page charges. This article must therefore be hereby marked *advertisement* in accordance with 18 U.S.C. Section 1734 solely to indicate this fact.

Received July 28, 2010; revised November 18, 2010; accepted December 14, 2010; published OnlineFirst February 23, 2011.

## References

1. Mathis JM, Stoff-Khalili MA, Curiel DT. Oncolytic adenoviruses—selective retargeting to tumor cells. Oncogene 2005;24:7775–91.
2. Ribacka C, Pesonen S, Hemminki A. Cancer, stem cells, and oncolytic viruses. Ann Med 2008;40:496–505.
3. Nemunaitis J, Tong AW, Nemunaitis M, Senzer N, Phadke AP, Bedell C, et al. A phase I study of telomerase-specific replication competent oncolytic adenovirus (telomelysin) for various solid tumors. Mol Ther 2010;18:429–34.
4. Li JL, Liu HL, Zhang XR, Xu JP, Hu WK, Liang M, et al. A phase I trial of intratumoral administration of recombinant oncolytic adenovirus overexpressing HSP70 in advanced solid tumor patients. Gene Ther 2009;16:376–82.
5. Freytag SO, Movsas B, Aref I, Stricker H, Peabody J, Pegg J, et al. Phase I trial of replication-competent adenovirus-mediated suicide gene therapy combined with IMRT for prostate cancer. Mol Ther 2007;15:1016–23.
6. Li Y, Yu DC, Chen Y, Amin P, Zhang H, Nguyen N, et al. A hepatocellular carcinoma-specific adenovirus variant, CV890, eliminates distant human liver tumors in combination with doxorubicin. Cancer Res 2001;61:6428–36.
7. Rodriguez R, Schuur ER, Lim HY, Henderson GA, Simons JW, Henderson DR. Prostate attenuated replication competent adenovirus (ARCA) CN706: a selective cytotoxic for prostate-specific antigen-positive prostate cancer cells. Cancer Res 1997;57:2559–63.
8. Matsubara S, Wada Y, Gardner TA, Egawa M, Park MS, Hsieh CL, et al. A conditional replication-competent adenoviral vector, Ad-OC-E1a, to cotarget prostate cancer and bone stroma in an experimental model of androgen-independent prostate cancer bone metastasis. Cancer Res 2001;61:6012–9.
9. Yamamoto M, Davydova J, Wang M, Siegal GP, Krasnykh V, Vickers SM, et al. Infectivity enhanced, cyclooxygenase-2 promoter-based conditionally replicative adenovirus for pancreatic cancer. Gastroenterology 2003;125:1203–18.
10. Kawashima T, Kagawa S, Kobayashi N, Shirakiya Y, Umeoka T, Teraishi F, et al. Telomerase-specific replication-selective virotherapy for human cancer. Clin Cancer Res 2004;10:285–92.
11. Taki M, Kagawa S, Nishizaki M, Mizuguchi H, Hayakawa T, Kyo S, et al. Enhanced oncolysis by a tropism-modified telomerase-specific replication-selective adenoviral agent OBP-405 ('Telomelysin-RGD'). Oncogene 2005;24:3130–40.
12. Watanabe T, Hioki M, Fujiwara T, Nishizaki M, Kagawa S, Taki M, et al. Histone deacetylase inhibitor FR901228 enhances the antitumor effect of telomerase-specific replication-selective adenoviral agent OBP-301 in human lung cancer cells. Exp Cell Res 2006;312:256–65.
13. Umeoka T, Kawashima T, Kagawa S, Teraishi F, Taki M, Nishizaki M, et al. Visualization of intrathoracically disseminated solid tumors in mice with optical imaging by telomerase-specific amplification of a transferred green fluorescent protein gene. Cancer Res 2004;64:6259–65.
14. Kishimoto H, Kojima T, Watanabe Y, Kagawa S, Fujiwara T, Uno F, et al. In vivo imaging of lymph node metastasis with telomerase-specific replication-selective adenovirus. Nat Med 2006;12:1213–9.
15. Hitt MM, Graham FL. Adenovirus E1A under the control of heterologous promoters: wide variation in E1A expression levels has little effect on virus replication. Virology 1990;179:667–78.
16. Takamizawa J, Konishi H, Yanagisawa K, Tomida S, Osada H, Endoh H, et al. Reduced expression of the let-7 microRNAs in human lung cancers in association with shortened postoperative survival. Cancer Res 2004;64:3753–6.
17. Michael MZ, SM OC, van Holst Pellekaan NG, Young GP, James RJ. Reduced accumulation of specific microRNAs in colorectal neoplasia. Mol Cancer Res 2003;1:882–91.
18. Slaby O, Svoboda M, Fabian P, Smerdova T, Knoflickova D, Bednarikova M, et al. Altered expression of miR-21, miR-31, miR-143 and miR-145 is related to clinicopathologic features of colorectal cancer. Oncology 2007;72:397–402.
19. Yanaihara N, Caplen N, Bowman E, Seike M, Kumamoto K, Yi M, et al. Unique microRNA molecular profiles in lung cancer diagnosis and prognosis. Cancer Cell 2006;9:189–98.
20. Johnson SM, Grosshans H, Shingara J, Byrom M, Jarvis R, Cheng A, et al. RAS is regulated by the let-7 microRNA family. Cell 2005;120:635–47.
21. Mizuguchi H, Kay MA. Efficient construction of a recombinant adenovirus vector by an improved in vitro ligation method. Hum Gene Ther 1998;9:2577–83.
22. Mizuguchi H, Kay MA. A simple method for constructing E1- and E1/E4-deleted recombinant adenoviral vectors. Hum Gene Ther 1999;10:2013–7.
23. Sakurai F, Kawabata K, Yamaguchi T, Hayakawa T, Mizuguchi H. Optimization of adenovirus serotype 35 vectors for efficient transduction in human hematopoietic progenitors: comparison of promoter activities. Gene Ther 2005;12:1424–33.
24. Maizel JV Jr, White DO, Scharff MD. The polypeptides of adenovirus. I. Evidence for multiple protein components in the virion and a comparison of types 2, 7A, and 12. Virology 1968;36:115–25.
25. Koizumi N, Kawabata K, Sakurai F, Watanabe Y, Hayakawa T, Mizuguchi H. Modified adenoviral vectors ablated for coxsackievirus-adenovirus receptor, alphav integrin, and heparan sulfate binding reduce in vivo tissue transduction and toxicity. Hum Gene Ther 2006;17:264–79.
26. Ishii-Watabe A, Uchida E, Iwata A, Nagata R, Satoh K, Fan K, et al. Detection of replication-competent adenoviruses spiked into recombinant adenovirus vector products by infectivity PCR. Mol Ther 2003;8:1009–16.

Published OnlineFirst February 23, 2011; DOI:10.1158/1078-0432.CCR-10-2008




27. Iorio MV, Visone R, Di Leva G, Donati V, Petrocca F, Casalini P, et al. MicroRNA signatures in human ovarian cancer. Cancer Res 2007;67:8699–707.
28. Mathonnet G, Fabian MR, Svitkin YV, Parsyan A, Huck L, Murata T, et al. MicroRNA inhibition of translation initiation in vitro by targeting the cap-binding complex eIF4F. Science 2007;317:1764–7.
29. Petersen CP, Bordeleau ME, Pelletier J, Sharp PA. Short RNAs repress translation after initiation in mammalian cells. Mol Cell 2006;21:533–42.
30. Pillai RS, Bhattacharyya SN, Artus CG, Zoller T, Cougot N, Basyuk E, et al. Inhibition of translational initiation by Let-7 MicroRNA in human cells. Science 2005;309:1573–6.
31. Cawood R, Chen HH, Carroll F, Bazan-Peregrino M, van Rooijen N, Seymour LW. Use of tissue-specific microRNA to control pathology of wild-type adenovirus without attenuation of its ability to kill cancer cells. PLoS Pathog 2009;5:e1000440.
32. Leja J, Nilsson B, Yu D, Gustafson E, Akerstrom G, Oberg K, et al. Double-detargeted oncolytic adenovirus shows replication arrest in liver cells and retains neuroendocrine cell killing ability. PLoS One 2010;5:e8916.
33. Ylosmaki E, Hakkarainen T, Hemminki A, Visakorpi T, Andino R, Saksela K. Generation of a conditionally replicating adenovirus based on targeted destruction of E1A mRNA by a cell type-specific MicroRNA. J Virol 2008;82:11009–15.
34. Brown BD, Gentner B, Cantore A, Colleoni S, Amendola M, Zingale A, et al. Endogenous microRNA can be broadly exploited to regulate transgene expression according to tissue, lineage and differentiation state. Nat Biotechnol 2007;25:1457–67.
35. Coulouarn C, Factor VM, Andersen JB, Durkin ME, Thorgeirsson SS. Loss of miR-122 expression in liver cancer correlates with suppression of the hepatic phenotype and gain of metastatic properties. Oncogene 2009;28:3526–36.
36. Bai S, Nasser MW, Wang B, Hsu SH, Datta J, Kutay H, et al. MicroRNA-122 inhibits tumorigenic properties of hepatocellular carcinoma cells and sensitizes these cells to sorafenib. J Biol Chem 2009;284:32015–27.
37. Gramantieri L, Ferracin M, Fornari F, Veronese A, Sabbioni S, Liu CG, et al. Cyclin G1 is a target of miR-122a, a microRNA frequently downregulated in human hepatocellular carcinoma. Cancer Res 2007;67:6092–9.
38. Edge RE, Falls TJ, Brown CW, Lichty BD, Atkins H, Bell JC. A let-7 MicroRNA-sensitive vesicular stomatitis virus demonstrates tumor-specific replication. Mol Ther 2008;16:1437–43.
39. Duerksen-Hughes P, Wold WS, Gooding LR. Adenovirus E1A renders infected cells sensitive to cytolysis by tumor necrosis factor. J Immunol 1989;143:4193–200.
40. Ramalingam R, Worgall S, Rafii S, Crystal RG. Downregulation of CXCR4 gene expression in primary human endothelial cells following infection with E1(-)E4(+) adenovirus gene transfer vectors. Mol Ther 2000;2:381–6.
41. Weitzman MD. Functions of the adenovirus E4 proteins and their impact on viral vectors. Front Biosci 2005;10:1106–17.

REPORT

Cell Cycle 10:16, 2737-2741; August 15, 2011; © 2011 Landes Bioscience

# Tumor-selective adenoviral-mediated GFP genetic labeling of human cancer in the live mouse reports future recurrence after resection

Hiroyuki Kishimoto,[1-3] Ryoichi Aki,[1,2] Yasuo Urata,[4] Michael Bouvet,[2] Masashi Momiyama,[1,2] Noriaki Tanaka,[3] Toshiyoshi Fujiwara[3] and Robert M. Hoffman[1,2,*]

[1]AntiCancer, Inc.; [2]Department of Surgery; University of California at San Diego; San Diego, CA USA; [3]Division of Surgical Oncology; Department of Surgery; Okayama University Graduate School of Medicine; Dentistry and Pharmaceutical Sciences; Okayama, Japan; [4]Oncolys BioPharma, Inc.; Tokyo, Japan

**Key words:** green fluorescent protein, adenovirus, cancer labeling, in situ, fluorescence-guided surgery, recurrence, detection

We have previously developed a telomerase-specific replicating adenovirus expressing GFP (OBP-401), which can selectively label tumors in vivo with GFP. Intraperitoneal (i.p.) injection of OBP-401 specifically labeled peritoneal tumors with GFP, enabling fluorescence visualization of the disseminated disease and real-time fluorescence surgical navigation. However, technical problems of removing all cancer cells still remain, even with fluorescence-guided surgery. In this study, we report that in vivo OBP-401 labeling of tumors with GFP before fluorescence-guided surgery reports cancer recurrence after surgery. Recurrent tumor nodules brightly expressed GFP, indicating that initial OBP-401-GFP labeling of peritoneal disease was genetically stable such that proliferating residual cancer cells still express GFP. In situ tumor labeling with a genetic reporter has important advantages over antibody and other non-genetic labeling of tumors, since residual disease remains labeled during recurrence and can be further resected under fluorescence guidance.



## Introduction

Green fluorescent protein (GFP) serves as a very bright genetic reporter to detect metastatic cancer in mouse models.[1-3] Initially, cancer cells were transduced in vitro with GFP using various types of genetic vectors and then implanted in mouse models. Potential clinical application of GFP became possible when it was demonstrated that retroviruses containing GFP could label disseminated cancer in situ in mouse models.[4] Subsequently, selective in vivo GFP labeling of tumors was performed with OBP-401, a replicating adenovirus[5,6] that contains a replication cassette with the human telomerase reverse transcriptase (hTERT) promoter driving the expression of the viral *E1* genes, and the inserted *GFP* gene. Virus replication and hence *GFP* gene expression occur only in the presence of an active telomerase, i.e., in malignant tissue.[6] The OBP-401 virus was first tested by injection directly into HT-29 human colon tumors, orthotopically implanted into the rectum in BALB/c *nu/nu* mice. Subsequent para-aortic lymph node metastasis was observed by laparotomy under fluorescence.[6] We then developed a major enhancement of cancer surgical navigation in orthotopic mouse models of cancer, using in vivo selective fluorescent tumor labeling with OBP-401 GFP. Bright GFP fluorescence clearly illuminated the tumor boundaries and facilitated detection of the smallest disseminated disease lesions.[7]

Fluorescence-guided surgical navigation with tumors labeled in vivo with OAP-401 GFP was demonstrated in nude mouse models that represent difficult surgical challenges for the resection of widely disseminated cancer. HCT-116, a model of intraperitoneal disseminated human colon cancer, was labeled by virus injection into the peritoneal cavity. A549, a model of pleural dissemination of human lung cancer, was labeled by OBP-401 virus administered into the pleural cavity. Only the malignant tissue fluoresced brightly in both models. Further, we showed that OBP-401 could visualize liver metastases by tumor-specific expression of the GFP gene after portal venous or i.v. administration. Selective metastatic tumor labeling with GFP and killing by systemic administration of telomerase-dependent adenoviruses suggesting that liver metastasis is also a candidate for fluorescence-guided surgery.[8]

However, even fluorescence-guided surgery may still result in residual disease. The present report demonstrates proliferating residual disease remains stably labeled with OBP-401 GFP and is readily detected for further resection, suggesting that genetic-reporter labeling of tumors has advantages over non-genetic labeling of tumors for fluorescence-guided surgery.

## Results and Discussion

**Labeling peritoneal carcinomatosis with OBP-401-GFP.** Peritoneal carcinomatosis was induced in the abdominal cavity of nude mice by i.p. implantation of HCT-116-RFP human colorectal cancer cells. Twelve days after implantation, 1 x $10^8$ PFU

*Correspondence to: Robert M. Hoffman; Email: all@anticancer.com
Submitted: 06/01/11; Revised: 06/09/11; Accepted: 06/10/11
DOI: 10.4161/cc.10.16.16756

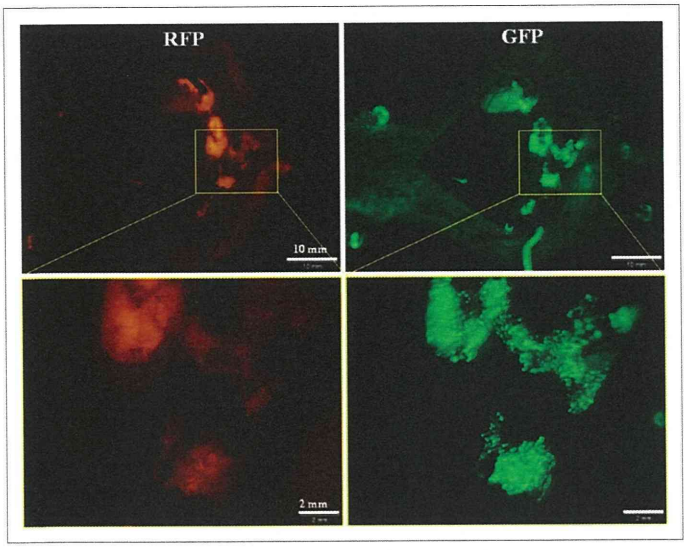


**Figure 1.** In situ genetic labeling of disseminated peritoneal carcinomatosis. Red fluorescence indicates HCT-116-RFP-expressing disseminated nodules (left). Peritoneal disseminated HCT116-RFP cells were labeled by GFP after i.p. injection of OBP-401 (right). Fluorescence imaging revealed co-localization of red and green fluorescence.

OBP-401 were injected intraperitoneally. Disseminated HCT-116-RFP nodules expressed GFP fluorescence induced by OBP-401 as well as the endogenous RFP fluorescence when imaged 5 d later (**Fig. 1**). RFP fluorescence was essentially coincident with that of GFP, indicating that i.p. injection of OBP-401 efficiently labeled disseminated tumors with GFP.

**Stability of OBP-401-GFP expression in tumors.** In order to determine stability of GFP expression in OBP-401 labeled tumors, HCT-116-RFP tumors were collected by peritoneal lavage from the abdominal cavity of mice 5 d after OBP-401 administration, put into culture in RPMI 1640 medium supplemented with 10% FBS and observed over time. Eight days after plating (13 d after viral administration), cancer cell colonies expressed both RFP and GFP (**Fig. 2**). The stability of GFP expression in OBP-401 labeled tumor cells suggests the potential of OBP-401 GFP labeling to detect recurrent tumors after attempted resection.

**Fluorescence-guided resection of disseminated peritoneal tumors labeled with OBP-401 GFP.** Five days after OBP-401 administration to mice with i.p. HCT-116, laparotomy was performed with the intent to remove all the intra-abdominal cancer using fluorescence-guided navigation under ketamine anesthesia (**Fig. 3A and B**). OBP-401 labeling and imaging made disseminated cancer nodules visible by GFP fluorescence, and complete resection was attempted (**Fig. 3C–E**). Tumors were efficiently resected, including those not visible under bright light, as we have previously reported in references 7 and 8.

**In vivo detection of recurrent OBP-402-GFP labeled tumors after fluorescence-guided surgery.** Tumors still recurred after attempted complete resection with fluorescence-guided surgery as visualized by GFP expression (**Fig. 4**). This result demonstrates that OBP-401 GFP labeling of peritoneal disseminated disease enables detection of tumor recurrence after fluorescence-guided surgery. Thus, OBP-401-GFP labeling is genetically stable and therefore proliferating residual disease continues to express GFP.

Tsien's laboratory has developed a method to label and visualize tumors during surgery using activatable cell-penetrating peptides (ACPPs), in which the fluorescently-labeled, polycationic cell-penetrating peptide (CPP) is coupled via a cleavable linker to a neutralizing peptide. Upon exposure to proteases expressed by tumors, the linker is cleaved, dissociating the inhibitory peptide and allowing the CPP to bind to and enter tumor cells. Animals whose tumors were resected with ACPPD guidance had better long-term tumor-free survival and overall survival than animals whose tumors were resected with traditional brightfield illumination only.[9]

Another approach to tumor labeling and fluorescence-guided surgery is with the use of labeled tumor-specific antibodies. A monoclonal antibody specific for CA19-9 was conjugated to a green fluorophore and delivered to tumor-bearing mice as a single intravenous (IV) dose. Intravital fluorescence imaging was used to localize metastatic pancreatic cancer in orthotopic mouse models 24 h after antibody administration. Using fluorescence imaging, the primary tumor was clearly visible at laparotomy, as were small metastases in the liver and spleen and on the peritoneum. The metastatic tumors, which were nearly impossible to see using standard brightfield imaging, demonstrated clear fluorescence under LED light excitation.[10]

We have also previously investigated the use of fluorophore-labeled anti-carcinoembryonic antigen (CEA) monoclonal antibody to aid in cancer visualization in nude mouse models of human colorectal and pancreatic cancer. Anti-CEA was conjugated with a green fluorophore. Subcutaneous, orthotopic primary and metastatic human pancreatic and colorectal tumors were easily visualized with fluorescence imaging after administration of conjugated anti-CEA. The fluorescence signal was detectable 30 min after systemic antibody delivery and remained present for 2 weeks, with minimal in vivo photobleaching after exposure to standard operating room lighting. Fluorescent anti-CEA administration improved ability to resect the labeled tumors under fluorescence guidance.[11]

Neither the ACPP nor labeled monoclonal antibodies, described above, involves genetic labeling of cancer cells, and thus recurrence would therefore not be detectable. In the present study, we selectively and efficiently labeled tumors with a genetic reporter, GFP, using a telomerase dependent adenovirus OBP-401. We demonstrated that tumors recurred after fluorescence-guided surgery and maintained GFP expression. Therefore, the detection of recurrence and future metastasis is possible with OBP-401 GFP labeling, since recurrent cancer cells stably express GFP, which is not possible with non-genetic labeling of tumors.

In clinical studies performed with OBP-401, circulating tumor cells (CTC) obtained from cancer patients were labeled with OBP-401 GFP ex vivo. OBP-401-GFP labeling greatly increased the detection of CTC.[12] Other targets for in vivo GFP labeling could include, for example, breast cancer emboli.[13] Specific labeling by GFP of cancer stem cells is also a promising approach.[14]

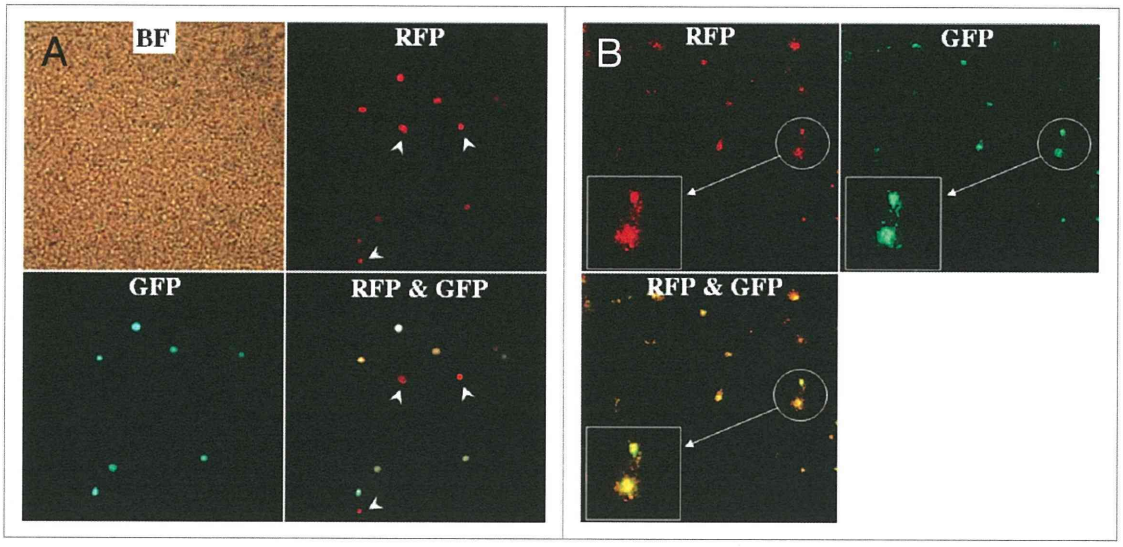


**Figure 2.** Genetic labeling of microscopic tumors. Cells collected by peritoneal lavage from the abdominal cavity of mice 5 d after OBP-401 treatment were plated and cultured with RPMI 1640 medium supplemented with 10% FBS. (A) Plating cells in the peritoneal lavage fluid (5 d after viral administration). Most RFP-expressing cancer cells expressed GFP fluorescence induced by OBP-401 as well, x200 magnification. White arrows: cells unlabeled with GFP. (B) 8 d after plating (i.e., 13 d after viral administration). Cancer cell colonies expressing RFP were observed in the culture dish under fluorescence microscopy. The cancer cells also expressed GFP induced by OBP-401. x40 magnification. Boxes highlight colonies indicated by white circles. Original magnification x100.

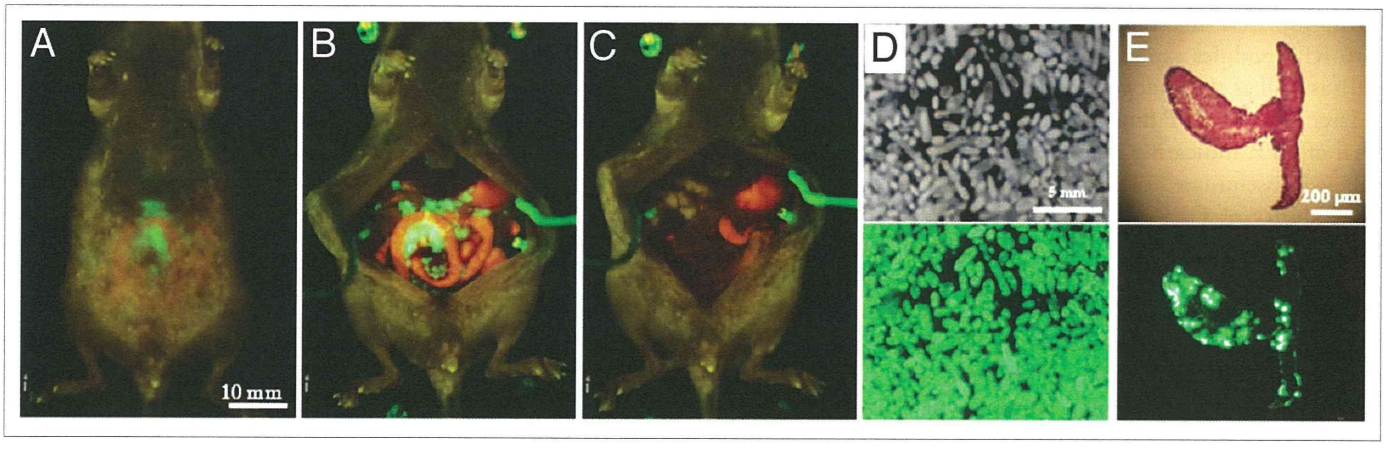


**Figure 3.** Fluorescence-guided resection of tumors labeled with GFP in situ. (A) Peritoneal disseminated nodules were labeled by GFP expression 5 d after OBP-401 virus administration. (B) Laparotomy was performed. (C) Disseminated nodules labeled with GFP were removed under GFP-guided surgical navigation. (D) Disseminated nodules removed under GFP-guided navigation. Top, bright field observation; bottom, fluorescent detection. (E) Section of disseminated nodules. Top, H&E section; bottom, frozen section with fluorescence detection.

Labeling of cancer stem cells is especially important, since at least some stem cells can now be imaged non-invasively.[15] The present report suggests the clinical potential of OBP-401 GFP labeling to improve the surgical outcome of cancer.

## Materials and Methods

**Recombinant adenovirus.** Telomerase-specific replication-selective adenovirus OBP-401, containing the *GFP* gene under the control of the CMV promoter with the hTERT promoter driving the *E1A* and *E1B* genes, was constructed and produced as previously described in references 5 and 6.

**Cell culture.** The human colorectal cancer cell line HCT-116 was cultured in RPMI 1640 medium supplemented with 10% FBS.

**Production of red fluorescent protein (RFP) retroviral vector.** For RFP retrovirus production, the *Hind*III/*Not*I fragment from pDsRed2 (Clontech), containing the full-length RFP cDNA, was inserted into the *Hind*III/*Not*I site of pLNCX2 (Clontech) containing the neomycin-resistance gene. PT67, an NIH3T3-derived packaging cell line (Clontech) expressing the viral envelope, was cultured in DMEM supplemented with 10% FBS. For vector production, PT67 packaging cells, at 70% confluence, were incubated with a precipitated mixture of LipofectAMINE reagent

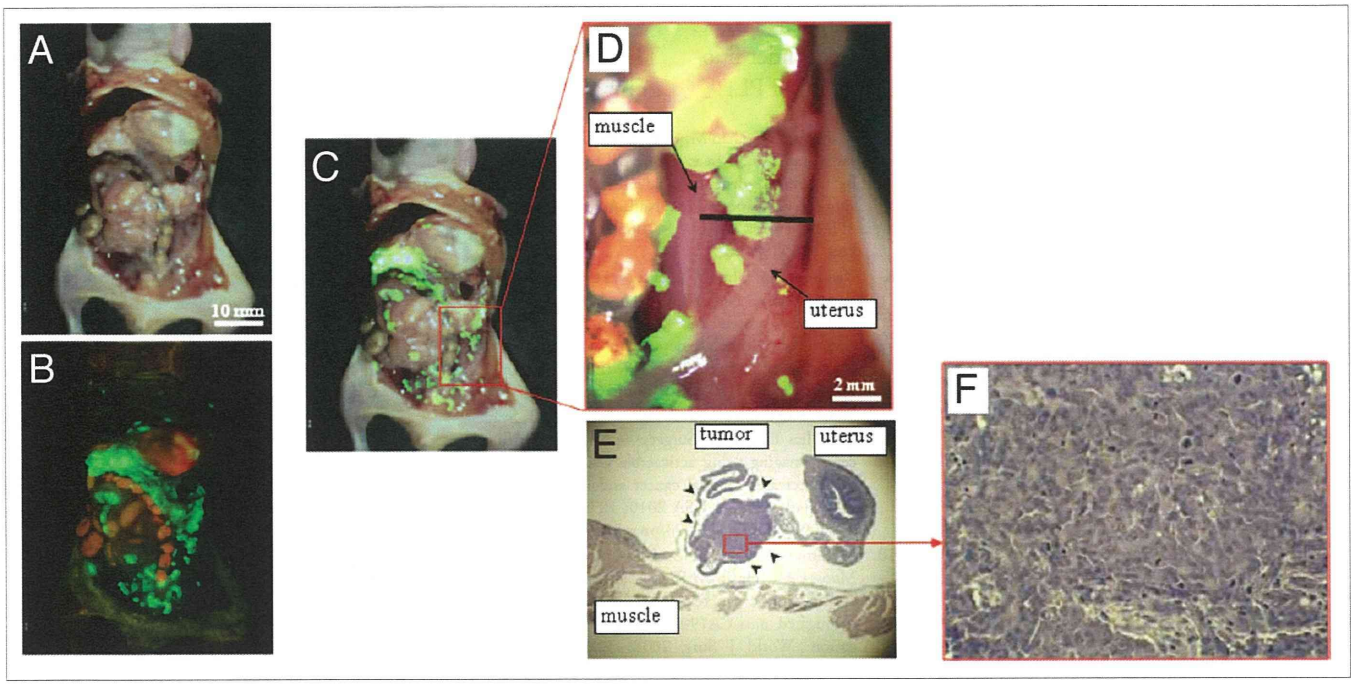


**Figure 4.** In vivo detection of recurrent tumors after fluorescence-guided surgery. (A) Brightfield observation several weeks after fluorescence-guided surgery of OBP-401 GFP-labeled tumors. Disseminated disease re-emerged. (B) Fluorescence observation of field observed by brightfield in (A). (C) Merge of (A and B). The red box outlines a region of (D) below. (D) Detail of the boxed region of (C). Black line indicates the direction of cross-sections. (E) Histologic sections stained with H&E showing that GFP-labeled lesions are recurrent tumor tissues (arrow heads). x40 magnification. (F) Detail of the boxed region of (E). x200 magnification.

(Life Technologies) and saturating amounts of pLNCX2-DsRed2 plasmid for 18 h. Fresh medium was replenished at this time. The cells were examined by fluorescence microscopy 48 h post-transduction. For selection of a clone producing high amounts of RFP retroviral vector (PT67-DsRed2), the cells were cultured in the presence of 200 to 1,000 μg/ml G418 (Life Technologies) for 7 d. The isolated packaging cell clone was termed PT67-DSRed2.[16]

**RFP gene transduction of cancer cells.** For RFP gene transduction, cancer cells were incubated with a 1:1 precipitated mixture of retroviral supernatants of PT67 cells and RPMI 1640 containing 10% FBS for 72 h. Fresh medium was replenished at this time. Tumor cells were harvested with trypsin/EDTA 72 h post-transduction and subcultured at a ratio of 1:15 into selective medium, which contained 200 μg/ml G418. To select brightly fluorescent cells, the level of G418 was increased up to 800 μg/ml in a stepwise manner. RFP-expressing cancer cells were isolated with cloning cylinders using trypsin/EDTA and were amplified by conventional culture methods in the absence of selective agent.[16]

**Mice.** Athymic nude mice were kept in a barrier facility under HEPA filtration and fed with autoclaved laboratory rodent diet. All animal studies were conducted in accordance with the principals and procedures outlined in the National Institute of Health Guide for the Care and Use of Laboratory Animals under Assurance Number A3873-1. All animal procedures were performed under anesthesia using s.c. administration of a ketamine mixture (10 μl ketamine HCL, 7.6 μl xylazine, 2.4 μl acepromazine maleate and 10 μl PBS).

**In vivo fluorescence imaging.** An Olympus OV100 Small Animal Imaging System (Olympus Corp., Tokyo, Japan) with macro and micro optics was used.[17] High-resolution images directly captured on a PC were processed and analyzed with the use of Adobe Photoshop Elements 4.0 software (Adobe).

**Peritoneal carcinomatosis model with HCT-116 human colon cancer cells implanted in nude mice.** Nude mice were intraperitoneally (i.p.) injected either with HCT-116 or HCT-116-RFP human colon cancer cells at a density of 3 x $10^6$ in 200 μl PBS. Twelve days after tumor cell inoculation, mice were injected i.p. with OBP-401 at a dose of 1 x $10^8$ PFU in 200 μl PBS. Five days after virus injection, the abdominal cavity was examined by fluorescence imaging, and mice were operated on with fluorescence guidance with the intent to resect all intra-abdominal tumor nodules under ketamine-induced anesthesia.

**Collection of microscopic tumors from peritoneal lavage fluid of OBP-401 treated mice.** Twelve days after nude mice were i.p. injected with HCT-116-RFP, 1 x $10^8$ PFU OBP-401 were injected intraperitoneally. Five days after virus injection, mice were instilled with 8 ml PBS intraperitoneally. The abdomen was gently massaged and the peritoneal fluid was carefully aspirated using a 22-gauge needle. Approximately 6 ml peritoneal lavage fluid (PLF) were obtained from most mice. After filtering the PLF with a 40 μm cell strainer (BD, Franklin Lakes, NJ) in order to collect only microscopic tumors and/or cancer cells in the abdominal cavity, 3 ml of PLF were cultured on 6-well tissue culture plates. After incubation for 1 h, supernatants were carefully aspirated and 3 ml RPMI 1640 medium, containing 10% FBS,

were added to each well. The cells were further incubated at 37°C in a humidified atmosphere of 5% $CO_2$ and observed under fluorescence microscopy at day 0 and day 8 after collection of PLF.


## Acknowledgments

This study was supported in part by National Cancer Institute grant CA132971 and CA142669.


## References


1. Chishima T, Miyagi Y, Wang X, Yamaoka H, Shimada H, Moossa AR, et al. Cancer invasion and micrometastasis visualized in live tissue by green fluorescent protein expression. Cancer Res 1997; 57:2042-7; PMID: 9158003.
2. Yang M, Baranov E, Jiang P, Sun FX, Li XM, Li L, et al. Whole-body optical imaging of green fluorescent protein-expressing tumors and metastases. Proc Natl Acad Sci USA 2000; 97:1206-11; PMID: 10655509; DOI: 10.1073/pnas.97.3.1206.
3. Hoffman RM. The multiple uses of fluorescent proteins to visualize cancer in vivo. Nat Rev Cancer 2005; 5:796-806; PMID: 16195751; DOI: 10.1038/nrc1717.
4. Hasegawa S, Yang M, Chishima T, Miyagi Y, Shimada H, Moossa AR, et al. In vivo tumor delivery of the green fluorescent protein gene to report future occurrence of metastasis. Cancer Gene Ther 2000; 7:1336-40; PMID: 11059691; DOI: 10.1038/sj.cgt.0237.
5. Fujiwara T, Kagawa S, Kishimoto H, Endo Y, Hioki M, Ikeda Y, et al. Enhanced antitumor efficacy of telomerase-selective oncolytic adenoviral agent OBP-401 with docetaxel: preclinical evaluation of chemovirotherapy. Int J Cancer 2006; 119:432-40; PMID: 16477640; DOI: 10.1002/ijc.21846.
6. Kishimoto H, Kojima T, Watanabe Y, Kagawa S, Fujiwara T, Uno F, et al. In vivo imaging of lymph node metastasis with telomerase-specific replication-selective adenovirus. Nat Med 2006; 12:1213-9; PMID: 17013385; DOI: 10.1038/nm1404.
7. Kishimoto H, Zhao M, Hayashi K, Urata Y, Tanaka N, Fujiwara T, et al. In vivo internal tumor illumination by telomerase-dependent adenoviral GFP for precise surgical navigation. Proc Natl Acad Sci USA 2009; 106:14514-7; PMID: 19706537; DOI: 10.1073/pnas.0906388106.
8. Kishimoto H, Urata Y, Tanaka N, Fujiwara T, Hoffman RM. Selective metastatic tumor labeling with green fluorescent protein and killing by systemic administration of telomerase-dependent adenoviruses. Mol Cancer Ther 2009; 8:3001-8; PMID: 19887549; DOI: 10.1158/1535-7163.MCT-09-0556.
9. Nguyen QT, Olson ES, Aquilera TA, Jiang T, Scadeng M, Ellies LG, et al. Surgery with molecular fluorescence imaging using activatable cell-penetrating peptides decreases residual cancer and improves survival. Proc Natl Acad Sci USA 2010; 107:4317-22; PMID: 20160097; DOI: 10.1073/pnas.0910261107.
10. McElroy M, Kaushal S, Luiken G, Talamini MA, Moossa AR, Hoffman RM, et al. Imaging of primary and metastatic pancreatic cancer using a fluorophore-conjugated anti-CA19-9 antibody for surgical navigation. World J Surg 2008; 32:1057-66; PMID: 18264829; DOI: 10.1007/s00268-007-9452-1.
11. Kaushal S, McElroy MK, Luiken GA, Talamini MA, Moossa AR, Hoffman RM, et al. Fluorophore-conjugated anti-CEA antibody for the intraoperative imaging of pancreatic and colorectal cancer. J Gastrointest Surg 2008; 12:1938-50; PMID: 18665430; DOI: 10.1007/s11605-008-0581-0.
12. Kojima T, Hashimoto Y, Watanabe Y, Kagawa S, Uno F, Kuroda S, et al. A simple biological imaging system for detecting viable human circulating tumor cells. J Clin Invest 2009; 119:3172-81; PMID: 19729837; DOI: 10.1172/JCI38609.
13. Mahooti S, Porter K, Alpaugh ML, Ye Y, Xiao Y, Jones S, et al. Breast carcinomatous tumoral emboli can result from encircling lymphovasculogenesis rather than lymphovascular invasion. Oncotarget 2010; 1:131-47; PMID: 21297224.
14. Runck LA, Kramer M, Ciraolo G, Lewis AG, Guasch G. Identification of epithelial label-retaining cells at the transition between the anal canal and the rectum in mice. Cell Cycle 2010; 9:3039-45; PMID: 20647777; DOI: 10.4161/cc.9.15.12437.
15. Uchugonova A, Hoffman RM, Weinigel M, Koenig K. Watching stem cells in the skin of living mice noninvasively. Cell Cycle 2011; 10:2017-20; PMID: 21558804; DOI: 10.4161/cc.10.12.15895.
16. Yamamoto N, Yang M, Jiang P, Xu M, Tsuchiya H, Tomita K, et al. Real-time imaging of individual fluorescent-protein color-coded metastatic colonies in vivo. Clin Exp Metastasis 2003; 20:633-8; PMID: 14669794; DOI: 10.1023/A:1027311230474.
17. Yamauchi K, Yang M, Jiang P, Xu M, Yamamoto N, Tsuchiya H, et al. Development of real-time subcellular dynamic multicolor imaging of cancer-cell trafficking in live mice with a variable-magnification whole mouse imaging system. Cancer Res 2006; 66:4208-14; PMID: 16618743; DOI: 10.1158/0008-5472.CAN-05-3927.

Gene Therapy (2012) 1-7

www.nature.com/gt

SHORT COMMUNICATION

# A simple detection system for adenovirus receptor expression using a telomerase-specific replication-competent adenovirus

T Sasaki[1], H Tazawa[2,3], J Hasei[1], S Osaki [1], T Kunisada[1,4], A Yoshida[1], Y Hashimoto[3], S Yano[3], R Yoshida[3], S Kagawa[3], F Uno[3], Y Urata[5], T Ozaki[1] and T Fujiwara[3]

Adenovirus serotype 5 (Ad5) is frequently used as an effective vector for induction of therapeutic transgenes in cancer gene therapy or of tumor cell lysis in oncolytic virotherapy. Ad5 can infect target cells through binding with the coxsackie and adenovirus receptor (CAR). Thus, the infectious ability of Ad5-based vectors depends on the CAR expression level in target cells. There are conventional methods to evaluate the CAR expression level in human target cells, including flow cytometry, western blotting and immunohistochemistry. Here, we show a simple system for detection and assessment of functional CAR expression in human tumor cells, using the green fluorescent protein (GFP)-expressing telomerase-specific replication-competent adenovirus OBP-401. OBP-401 infection induced detectable GFP expression in CAR-expressing tumor cells, but not in CAR-negative tumor cells, nor in CAR-positive normal fibroblasts, 24 h after infection. OBP-401-mediated GFP expression was significantly associated with CAR expression in tumor cells. OBP-401 infection detected tumor cells with low CAR expression more efficiently than conventional methods. OBP-401 also distinguished CAR-positive tumor tissues from CAR-negative tumor and normal tissues in biopsy samples. These results suggest that GFP-expressing telomerase-specific replication-competent adenovirus is a very potent diagnostic tool for assessment of functional CAR expression in tumor cells for Ad5-based antitumor therapy.

*Gene Therapy* advance online publication, 12 January 2012; doi:10.1038/gt.2011.213

**Keywords:** oncolytic virus; adenovirus; telomerase; sarcoma; GFP

## INTRODUCTION

Adenovirus serotype 5 (Ad5) is widely and frequently used as an effective vector in cancer gene therapy and oncolytic virotherapy.[1-3] Adenovirus-mediated transgene transduction is a highly efficient method for induction of ectopic transgene expression in tumor cells.[1,2] The p53 tumor suppressor gene, which is a potential therapeutic transgene that may induce a very strong antitumor effect, has been transduced into tumor cells using a replication-deficient adenovirus vector (Ad-p53, Advexin, Intorgen Therapeutics, Inc., Austin, TX, USA), and Ad-p53 has been reported to induce an antitumor effect in clinical studies.[4-7] Recently, an Ad5-based replication-competent oncolytic adenovirus has been developed as a promising anticancer reagent for induction of tumor-specific cell lysis.[8,9] Ad5-based vectors infect human target cells through binding with the coxsackie and adenovirus receptor (CAR).[10] Thus, the infection efficiency of Ad5-based vectors mainly depends on the CAR expression level in tumor tissues.[11-17] Increased CAR expression has been frequently shown in tumor cells in various organs such as the brain,[18] thyroid,[19] esophagus,[20] gastrointestinal tract,[21] prostate,[14] bone and soft tissues.[22-24] However, tumor cells often show reduced CAR expression following tumor progression.[18,21,25,26] Decreased CAR expression has also been shown in tumor tissues after repeated injection of Ad-p53.[27,28] It is therefore necessary to assess the CAR expression level of target tumor tissues before and after Ad5-based cancer gene therapy and oncolytic virotherapy.

There are some conventional methods for evaluation of the CAR expression level in tumor tissues, such as flow cytometry, immunohistochemistry, western blotting and reverse transcription (RT)-PCR . Flow cytometry is mainly used to detect CAR-positive human tumor cell lines.[13,24,28,29] Immunohistochemistry is frequently used to assess CAR expression in various human tumor tissues.[11,14,20,23,25] Western blotting is usually performed to confirm the expression of many types of proteins including CAR in molecular biological experiments. Quantitative RT-PCR is also a useful method for evaluation of the mRNA expression of CAR.[18,22] Although these conventional methods can detect CAR expression in tumor tissues, it still remains unclear whether Ad5-based vectors really infect target tumor cells through binding with the CAR that is detected using conventional methods. Therefore, the development of a novel method for assessment of the level of expression of functional CAR in tumor tissues, which is what the Ad5-based vectors really bind, is required for Ad5-based anticancer therapy.

We previously developed a telomerase-specific replication-competent adenovirus OBP-301 (Telomelysin, Oncolys BioPharma, Inc., Tokyo, Japan) that drives the *E1A* and *E1B* genes under the human telomerase reverse transcriptase (*hTERT*) promoter.[8,29-31] OBP-301 infects both normal and tumor cells that express CAR, but replicates only in CAR-positive tumor cells in a telomerase-dependent manner. Furthermore, we recently generated a green fluorescent protein (GFP)-expressing telomerase-specific replication-

[1]Department of Orthopaedic Surgery, Okayama University Graduate School of Medicine, Dentistry and Pharmaceutical Sciences, Okayama, Japan; [2]Center for Gene and Cell Therapy, Okayama University Hospital, Okayama, Japan; [3]Department of Gastroenterological Surgery, Okayama University Graduate School of Medicine, Dentistry and Pharmaceutical Sciences, Okayama, Japan; [4]Department of Medical Materials for Musculoskeletal Reconstruction, Okayama University Graduate School of Medicine, Dentistry and Pharmaceutical Sciences, Okayama, Japan and [5]Oncolys BioPharma, Inc., Tokyo, Japan. Correspondence: Professor T Fujiwara, Department of Gastroenterological Surgery, Okayama University Graduate School of Medicine, Dentistry and Pharmaceutical Sciences, 2-5-1 Shikata-cho, Kita-ku, Okayama 700-8558, Japan.
E-mail: toshi_f@md.okayama-u.ac.jp
Received 15 July 2011; revised 7 November 2011; accepted 5 December 2011

competent adenovirus OBP-401, which induces ectopic GFP expression in tumor cells, but not in normal cells.[32] OBP-401 infection efficiently induces GFP expression in metastatic tumor cells at regional lymph nodes[32] and liver,[33] circulating tumor cells in blood flow[34] and disseminated tumor cells in the abdominal cavity.[35] These results suggest that OBP-401 is a highly sensitive tool for the detection of tumor cells. Furthermore, Ad5-based OBP-401 would also be useful for induction of GFP expression in CAR-positive tumor cells, but not in CAR-negative tumor cells.

In the present study, we evaluated whether induction of GFP expression by OBP-401 infection is associated with CAR expression in tumor cells. OBP-401-mediated GFP induction was further examined in xenograft tumor tissues that have different levels of CAR expression and in surrounding normal tissues.

## RESULTS AND DISCUSSION

### Assessment of an OBP-401 infection protocol for the detection of CAR-positive tumor cells

We recently demonstrated that the level of CAR expression that was detected using flow cytometry was significantly associated with OBP-301-mediated cytopathic activity in human bone and soft tissue sarcoma cells.[29] Furthermore, OBP-401 infection has been shown to induce GFP expression 24 h after infection of human sarcoma cells.[34] To evaluate whether GFP expression that is induced by OBP-401 infection is associated with CAR expression in tumor cells, we used three human sarcoma cell lines (OST, NMFH-1 and OUMS-27) that have different levels of CAR expression, as previously reported.[29] Flow cytometric analysis confirmed that OST cells showed detectable CAR expression, whereas cells of the NMFH-1 and OUMS-27 sarcoma cell lines had no detectable CAR expression (Figure 1a).

To determine suitable conditions for OBP-401 infection in order to detect CAR-positive tumor cells, OST sarcoma cells were infected with OBP-401 at multiplicity of infections (MOIs) of 1, 10 and 100 plaque-forming units (PFU) per cell over 24 h (Figure 1b and c). Twelve hours after infection, only OBP-401 infection at an MOI of 100 had induced GFP expression in all of the OST cells. Twenty-four hours after infection, OBP-401 infection at MOIs of 10 and 100 had induced ectopic GFP expression in all of the OST cells, whereas OBP-401 infection at an MOI of 1 had induced GFP expression in about 80% of the OST cells. These results indicate that OBP-401 infection at an MOI of greater than 10 is necessary to efficiently detect CAR-positive tumor cells 24 h after infection.

To subsequently determine a suitable condition for OBP-401 infection that would exclude CAR-negative tumor cells, the NMFH-1 and OUMS-27 sarcoma cells that do not express CAR were infected with OBP-401 at MOIs of 10 and 100 for 60 h (Figures 1d and e). NMFH-1 cells expressed GFP at 24 and 48 h after OBP-401 infection at MOIs of 100 and 10, respectively. In contrast, OUMS-27 cells exhibited no GFP expression after OBP-401 infection. To investigate the different GFP expression between these CAR-negative tumor cells, expression of integrins, $\alpha v\beta 3$ and $\alpha v\beta 5$, was further examined by flow cytometry. NMFH-1 cells showed twofold higher expression of integrin $\alpha v\beta 3$ compared with OUMS-27 cells, whereas $\alpha v\beta 5$ expression was similar in these cells (Supplementary Figure S1a). These results indicate that OBP-401 infection at an MOI of 10 for 24 h is a suitable protocol for distinguishing CAR-negative tumor cells from CAR-positive tumor cells, when CAR-negative tumor cells express integrin molecules.

### Relationship between OBP-401-induced GFP expression and CAR expression

To evaluate whether OBP-401-induced GFP expression correlates with CAR expression in tumor cells, six human sarcoma cell lines (OST, U2OS, NOS-10, MNNG/HOS, NMFH-1 and OUMS-27) and normal human lung fibroblasts (NHLF) cells that have different levels of CAR expression (Figure 1a and Supplementary Figure S1b) were infected with OBP-401 at an MOI of 10 for 24 h, and the GFP-positive cells in each cell type were analyzed under fluorescence microscopy (Figures 2a and b). OBP-401 infection-induced GFP expression from 12 h after infection and, after 24 h, more than 40% of all CAR-positive tumor cells (OST, U2OS, NOS-10 and MNNG/HOS) were detected as GFP-positive cells. However, no GFP-positive cells were detected in the CAR-negative tumor cells (NMFH-1, OUMS-27), or in the normal NHLF cells, 24 h after infection. Furthermore, OBP-401-mediated GFP induction in CAR-positive tumor cells was suppressed by blocking CAR proteins with anti-CAR antibody (Supplementary Figure S2). To assess the GFP expression level in all tumor and normal cells in a more quantitative manner, we quantified the level of GFP fluorescence in each cell type 24 h after infection using a fluorescence microplate reader (Figure 2c). We also quantified the level of CAR expression in these cells by calculating the mean fluorescence intensity in flow cytometric analysis (Figure 2d). GFP fluorescence was detected in CAR-positive tumor cells, but not in either CAR-negative tumor cells or in CAR-positive normal cells. There was a significant relationship between the CAR expression level and the GFP fluorescence level ($r = 0.885$; $P = 0.019$) (Figure 2e). These results indicate that OBP-401-mediated GFP expression is highly associated with CAR expression in tumor cells.

### Comparison of the potential of OBP-401-mediated GFP induction and of conventional methods for CAR detection

To estimate the potential of OBP-401-mediated GFP induction for the detection of CAR-positive tumor cells, we compared the above protocol using OBP-401 with western blot analysis and immunocytochemistry. CAR expression was detected in OST, U2OS and NOS-10 sarcoma cells, but not in CAR-positive MNNG/HOS sarcoma cells, using western blot analysis (Supplementary Figure S3a). In contrast, only OST cells displayed a positive CAR signal using immunocytochemistry, whereas the CAR signal of the other three CAR-positive tumor cells was almost as weak as that from CAR-negative tumor cells (Supplementary Figure S3b). CAR expression was also not detected in CAR-positive NHLF cells by either western blot analysis or by immunocytochemistry. These results suggest that the GFP induction protocol using OBP-401 is more sensitive for the detection of CAR-positive tumor cells than conventional methods.

OBP-401-mediated GFP induction was detected in MNNG/HOS sarcoma cells that expressed a low level of CAR (Figure 2c), although neither western blot analysis nor immunocytochemistry detected CAR in these cells (Supplementary Figure S3). Furthermore, although conventional methods may be able to detect high CAR expression in tumor cells, whether the CAR expression that is detected by conventional methods is really functional for binding with Ad5-based vectors still remains unclear. In contrast, as OBP-401 is an Ad5-based vector that expresses a fluorescent *GFP* gene, OBP-401-induced GFP expression directly proves that the CAR that is expressed is functional for Ad5-based vector binding. Thus, the OBP-401-mediated GFP induction strategy is a potential diagnostic method that can efficiently and directly assess functional CAR expression in tumor cells.

### OBP-401-mediated GFP induction in xenograft tumor and normal tissues with different CAR expression

Finally, to investigate the potential of the OBP-401-mediated method for the detection of CAR expression in tumor and normal tissues, we used this method to analyze CAR expression of human xenograft tumor tissues, that do or do not express CAR, as well as of surrounding normal muscle tissues, which have been previously shown to lose CAR expression.[36] CAR-positive OST sarcoma cells or CAR-negative OUMS-27 sarcoma cells were inoculated into nude

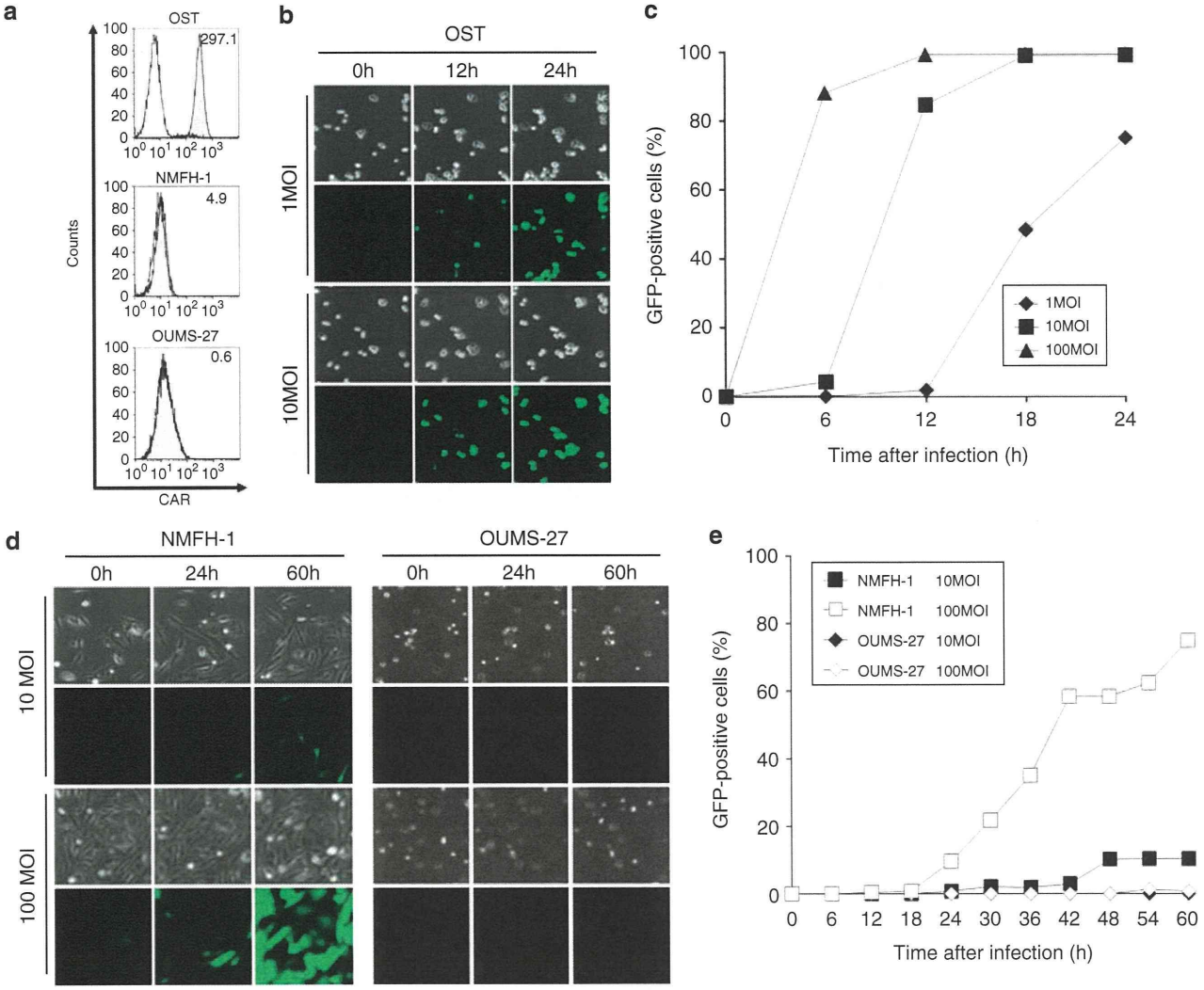


**Figure 1.** Establishment of a suitable protocol for the detection of CAR expression using OBP-401. (**a**) The level of CAR expression on three human sarcoma cell lines (OST, NMFH-1 and OUMS-27) was analyzed using flow cytometry. The cells were incubated with a monoclonal anti-CAR (RmcB) antibody and the signal was detected using a fluorescent isothiocyanate (FITC)-labeled secondary antibody. The mean fluorescence intensity (MFI), which is a measure of CAR and integrin expression, was calculated for each cell and is shown at the top right of each graph. (**b**) Time-lapse images of OST cells, which displayed the highest CAR expression, were recorded for 24 h after OBP-401 infection at MOIs of 1 and 10 PFU per cell. Representative images taken at the indicated time points and MOIs show cell morphology that was analyzed using phase-contrast microscopy (top panels) and GFP expression that was analyzed using fluorescence microscopy (bottom panels). Original magnification: ×80. (**c**) The percentage of GFP-positive cells was counted in OST cells at the indicated time points after OBP-301 infection at MOIs of 1, 10 and 100 PFU per cell. (**d**) Time-lapse images of non-CAR-expressing OUMS-27 and NMFH-1 cells were recorded for 60 h after OBP-401 infection at MOIs of 10 and 100 PFU per cell. Representative images taken at the indicated time points and MOIs show cell morphology that was analyzed using phase-contrast microscopy (top panels) and GFP expression that was analyzed using fluorescence microscopy (bottom panels). Original magnification: ×80. (**e**) The percentage of OUMS-27 and NMFH-1 GFP-positive cells was counted at the indicated time points after OBP-301 infection at MOIs of 10 and 100 PFU per cell.

mice to develop xenograft tumors. After resection of the OST tumors, the OUMS-27 tumors and normal muscle tissue, the tissues were subjected to the protocol for OBP-401-mediated GFP induction using a three-step procedure (Figure 3a) as follows; step 1: OBP-401 infection for 24 h, step 2: washing with PBS and step 3: observation under a fluorescence microscope. As shown in Figure 3b, OBP-401 infection-induced GFP expression in CAR-positive OST tumor tissues, but not in CAR-negative OUMS-27 tumor tissues or in normal muscle tissue. These results suggest that OBP-401-mediated GFP induction is a simple and useful method for the detection of CAR expression by tumor tissues.

Flow cytometry is a highly sensitive conventional method for the detection of cell surface CAR expression, which is associated with the therapeutic efficacy of Ad5-based vectors in tumor cells.[13,24,28,29] However, as many tumor cells tightly bind to each other or to normal stromal cells within tumor tissues, the preparation of single tumor cells is not easy, and therefore flow cytometry is an inadequate method for the detection of CAR expression in tumor tissues. In contrast, the preparation of single tumor cells is not necessary for the OBP-401-mediated GFP induction protocol. Furthermore, assay of OBP-401-induced GFP expression was more sensitive than flow cytometry (Figure 2d) in distinguishing CAR-positive normal cells from CAR-positive tumor cells (Figure 2c). Thus, the OBP-401-mediated GFP induction method is a simple and tumor-specific system for the detection of CAR expression in tumor tissues.

Fluorescent proteins including GFP have great potentials to visualize tumor cells in real time on the *in vivo* setting.[37,38]

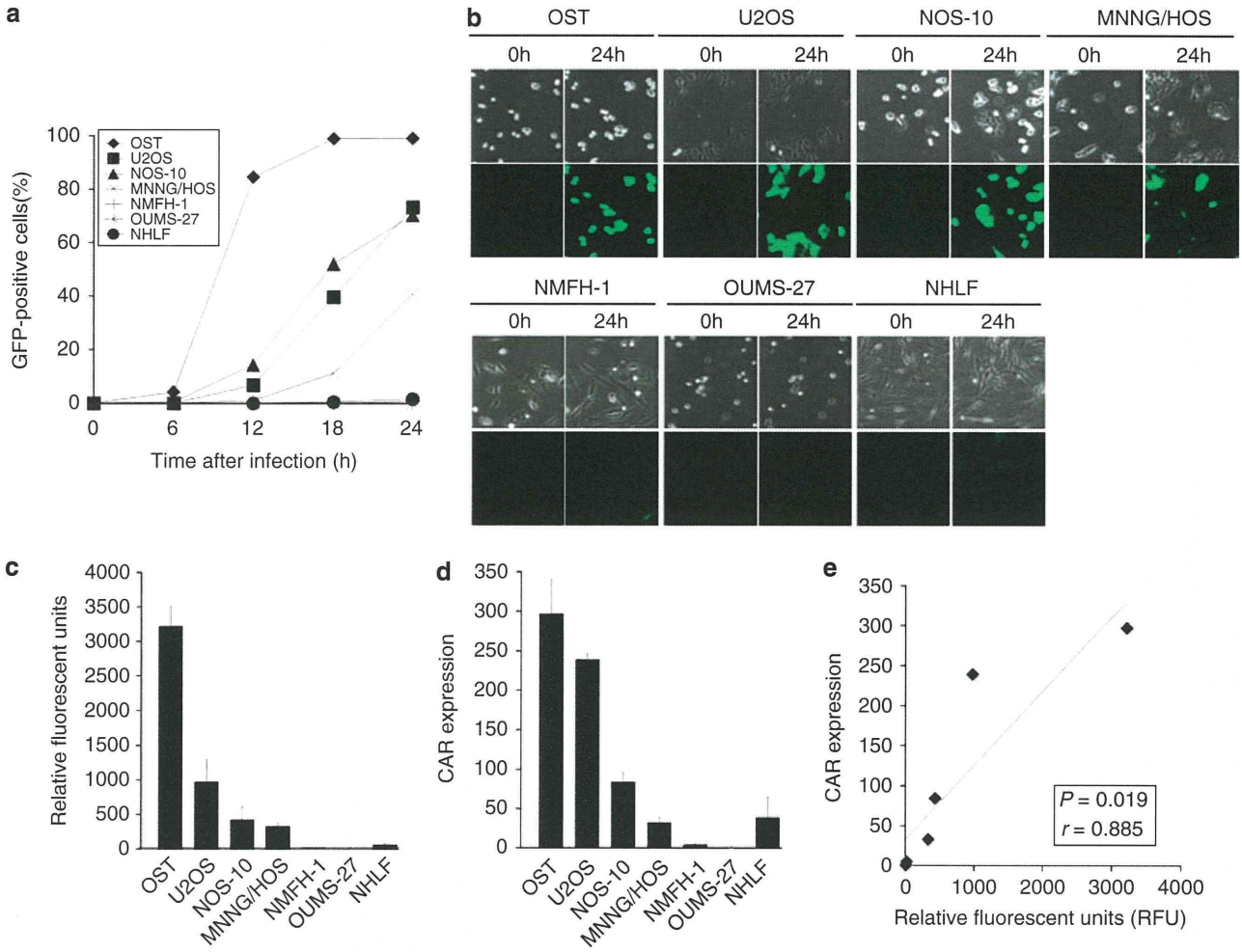


**Figure 2.** *In vitro* CAR-dependent GFP expression induced by OBP-401 infection. (**a**) The percentage of GFP-positive cells in all tumor and normal cells was counted at the indicated time points after OBP-301 infection at an MOI of 10 PFU per cell. (**b**) Time-lapse images of all tumor and normal cells were recorded for 24 h after infection with OBP-401 at an MOI of 10 PFU per cell. Representative images taken at the indicated time points show cell morphology that was analyzed using phase-contrast microscopy (top panels) and GFP expression that was analyzed using fluorescence microscopy (bottom panels). Original magnification: × 80. (**c**) Quantitative assessment of the level of GFP fluorescence in all tumor and normal cells 24 after OBP-401 infection at an MOI of 10 PFU per cell, using a fluorescent microplate reader with excitation/emission at 485 nm/528 nm. The intensity of GFP fluorescence was evaluated based on the brightness determinations used as relative fluorescence units (RFU). (**d**) The mean fluorescent intensity (MFI) of (CAR) expression on human sarcoma cells and normal fibroblasts. The cells were incubated with a monoclonal anti-CAR (RmcB) antibody, followed by a FITC-labeled secondary antibody, and were analyzed using flow cytometry. (**e**) Relationship between the level of GFP fluorescence and CAR expression in all tumor and normal cells after OBP-401 infection. The slope represents the inverse correlation between these two factors. Statistical significance was determined as $P<0.05$, after analysis of Pearson's correlation coefficient.

We previously reported that OBP-401 can efficiently induce GFP expression in small populations of metastatic tumor cells at various regions *in vivo*.[32-35] In this study, we further demonstrated that OBP-401-mediated GFP expression provides us the important information for detection of CAR-positive tumor cells. OBP-401 with *hTERT* gene promoter-induced GFP expression in CAR-positive tumor cells with telomerase activity, but not CAR-positive normal cells without telomerase activity (Figure 2c). There was significant relationship between the CAR expression and the GFP expression in tumor cells (Figure 2d). Among the four CAR-positive tumor cells, U2OS cells showed low GFP expression compared with high CAR expression (Figure 1a and 2c). As we recently reported that U2OS cells showed low *hTERT* mRNA expression, the low activity of *hTERT* gene promoter in tumor cells would affect OBP-401-mediated GFP expression. However, as various types of human cancer cells frequently show high telomerase activities,[39] OBP-401-mediated GFP induction system would be widely useful method to evaluate CAR expression in tumor cells.

Previous reports have suggested that *ex vivo* infection of human cancer specimens with a GFP-expressing replication-deficient adenovirus[40] or a replication-selective oncolytic adenovirus[41] is a useful method for assessment of the transduction efficacy or cytopathic activity, respectively, of Ad5-based vectors in individual tumor tissues. In this study, we confirmed that the GFP-expressing telomerase-specific oncolytic adenovirus OBP-401 is useful for detection of CAR-positive tumor tissues through induction of GFP expression (Figure 3b). Interestingly, OBP-401-infected OST tumor tissues showed heterogenous GFP expression (Figure 3b), although GFP expression was induced in all OBP-401-infected OST cells *in vitro* (Figure 2b). Our finding of heterogenous GFP expression in tumor tissues, which indicates heterogenous CAR expression, is consistent with a previously reported heterogeneity in CAR expression.[42] As several factors such as hypoxia[43] and cell cycle status[44] have been suggested to affect CAR expression in tumor cells, factors in the tumor microenvironment may be involved in the heterogenous CAR expression in tumor cells.

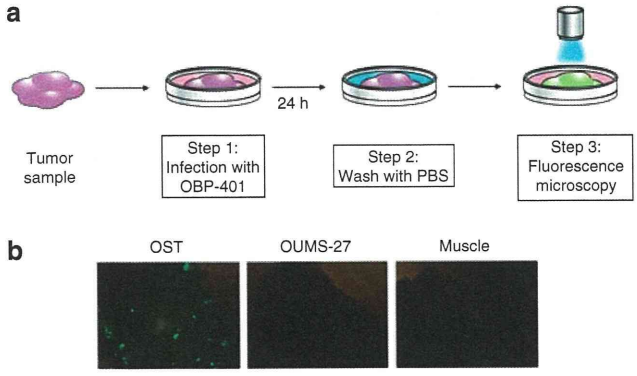


**Figure 3.** A simple method for detection of CAR expression in tumor tissues using OBP-401 infection. (**a**) Outline of the 3-step procedure; step 1: infection with OBP-401, step 2: washing with PBS and step 3: observation under a fluorescence microscope. Tumor tissues ($2 \times 2 \times 2\,mm^3$) were infected with OBP-401 at a concentration of $2.4 \times 10^6$ PFU for 24 h, were washed with PBS and were observed using fluorescence microscopy. (**b**) Assessment of GFP expression in the CAR-positive OST tumor (left panel), the CAR-negative OUMS-27 tumor (middle panel) and normal muscle tissues (right panel) under a fluorescence microscope. Original magnification: $\times 30$.

Furthermore, as OBP-401 induces tumor-specific GFP expression, normal stromal or epithelial cells may be involved in heterogenous GFP expression in tumor tissues.

In conclusion, we have demonstrated that the GFP-expressing telomerase-specific replication-competent adenovirus OBP-401 is a promising fluorescence imaging tool for the detection of functional and tumor-specific CAR expression in tumor tissues. OBP-401-mediated GFP induction is a simple and highly sensitive method for analysis of tumor cells compared with conventional methods. This novel CAR detection system using OBP-401 has the potential of being widely applicable to assessment of predictive biomarkers for Ad5-based vector-mediated anticancer therapy.

## MATERIALS AND METHODS

### Cell lines

The human osteosarcoma cell line OST was kindly provided by Dr Satoru Kyo (Kanazawa University, Ishikawa, Japan). The human osteosarcoma cell line U2OS and the transformed embryonic kidney cell line 293 were obtained from the American Type Culture Collection (ATCC; Manassas, VA, USA). The human osteosarcoma cell line NOS-10[45] and the human malignant fibrous histiocytoma cell line NMFH-1[46] were kindly provided by Dr Hiroyuki Kawashima (Niigata University, Niigata, Japan). The human osteosarcoma cell line MNNG/HOS was purchased from DS Pharma Biomedical (Osaka, Japan). The chondrosarcoma cell line OUMS-27 was previously established in our laboratory.[47] The normal human lung fibroblast cell line NHLF was obtained from TaKaRa Biomedicals (Kyoto, Japan). These cells were propagated as monolayer cultures in the medium recommended by the manufacturer. All media were supplemented with 10% heat-inactivated fetal bovine serum, 100 units $ml^{-1}$ penicillin and 100 $\mu g\,ml^{-1}$ streptomycin. The cells were maintained at 37 °C in a humidified atmosphere containing 5% $CO_2$.

### Recombinant adenoviruses

We previously generated and characterized OBP-401, which is a telomerase-specific replication-competent adenovirus variant, in which the *hTERT* promoter element drives the expression of *E1A* and *E1B* genes that are linked to an internal ribosome entry site, and in which the *GFP* gene is inserted into the E3 region under a cytomegalovirus promoter.[32,34] The virus was purified by ultracentrifugation using cesium chloride step gradients. Viral titers were determined by a plaque-forming assay using 293 cells and viruses were stored at −80 °C.

### Flow cytometry

The cells ($5 \times 10^5$ cells) were labeled with the mouse monoclonal anti-CAR (RmcB; Upstate Biotechnology, Lake Placid, NY, USA) antibody for 30 min at 4 °C. The cells were then incubated with fluorescent isothiocyanate-conjugated rabbit anti-mouse IgG second antibody (Zymed Laboratories, San Francisco, CA, USA) and were analyzed using flow cytometry (FACS Array; Becton Dickinson, Mountain View, CA, USA). The mean fluorescence intensity of CAR for each cell line was determined by calculating the differences between the mean fluorescence intensity in antibody-treated and non-treated cells in triplicate experiments.

### Time-lapse confocal laser microscopy

The cells ($1 \times 10^5$ cells per dish) were seeded in 35 mm glass-based dishes 20 h before virus infection. OST cells were infected with OBP-401 at an MOI of 1, 10 or 100 PFU per cell for 24 h. NMFH-1 and OUMS-27 cells were infected with OBP-401 at an MOI of 10 or 100 PFU per cell for 60 h. Other cells were infected with OBP-401 at an MOI of 10 PFU per cell for 24 h. Phase-contrast and fluorescence time-lapse recordings were obtained to concomitantly analyze cell morphology and GFP expression using an inverted FV10i confocal laser scanning microscopy (OLYMPUS; Tokyo, Japan). Photographic images were taken every 5 min. The percentage of GFP-positive cells in each field was calculated using the formula: the number of CAR-positive cells / the total number of CAR-positive and CAR-negative cells $\times 100$.

### Fluorescence microplate assay

The cells ($5 \times 10^3$ cells per well) were seeded on 96-well black bottomed culture plates and were incubated for 20 h before virus infection. The cells were infected with OBP-401 at an MOI of 10 for 24 h. The level of expression of GFP fluorescence was measured using a fluorescent microplate reader (DS Pharma Biomedical; Osaka, Japan) with excitation/emission at 485 nm/528 nm. The mean expression of GFP fluorescence in each cell was calculated in triplicate experiments, as previously reported.[34]

### Animal experiments

Animal experimental protocols were approved by the Ethics Review Committee for Animal Experimentation of Okayama University School of Medicine. OST and OUMS-27 cells ($5 \times 10^6$ cells per site) were inoculated into the flank of female athymic nude mice aged 6 to 7 weeks (Charles River Laboratories, Wilmington, MA, USA). Palpable tumors developed within 14 to 21 days and were permitted to grow to ~5 to 6 mm in diameter. At that stage, tumor and normal muscle tissues were resected. The tumor and normal tissues ($2 \times 2 \times 2\,mm^3$) were placed in 96-well plates with culture medium. As single tumor cell is about 10 $\mu$m in diameter, we considered that there are $2.4 \times 10^5$ cells on the surface area of each sample tissue. Then, we infected each sample tissue with $2.4 \times 10^6$ PFU (10 MOI per sample) of OBP-401 for 24 h. After washing with PBS, tumor and normal tissues were again placed in 96-well plates with culture medium and analyzed using an inverted fluorescence microscope (OLYMPUS).

### Statistical analysis

Data are expressed as means ± s.d. Student's *t*-test was used to compare differences between groups. Pearson's product-moment correlation coefficients were calculated using PASW statistics software version 18 (SPSS Inc., Chicago, IL, USA). Statistical significance was defined as when the *P* value was less than 0.05.

## ABBREVIATIONS

Ad5, Adenovirus serotype 5; CAR, coxsackie and adenovirus receptor; GFP, green fluorescent protein; RT-PCR, reverse transcription-polymerase chain reaction; hTERT, human telomerase reverse transcriptase; MOI, multiplicity of infection;

PFU, plaque-forming unit; IRES, internal ribosome entry site; FITC, fluorescent isothiocyanate; MFI, mean fluorescence intensity.

## CONFLICT OF INTEREST

Y Urata is an employee of Oncolys BioPharma, Inc., the manufacturer of OBP-401 (Telomescan). The remaining authors declare no conflict of interest.

## ACKNOWLEDGEMENTS

We thank Dr Satoru Kyo (Kanazawa University) for providing the OST cells; Dr Hiroyuki Kawashima (Niigata University) for providing the NOS-10 and NMFH-1 cells; and Tomoko Sueishi for her excellent technical support. This study was supported by grants-in-Aid from the Ministry of Education, Science and Culture, Japan and grants from the Ministry of Health and Welfare, Japan.

## REFERENCES

1 Kanerva A, Hemminki A. Adenoviruses for treatment of cancer. *Ann Med* 2005; **37**: 33-43.
2 Rein DT, Breidenbach M, Curiel DT. Current developments in adenovirus-based cancer gene therapy. *Future Oncol* 2006; **2**: 137-143.
3 Yamamoto M, Curiel DT. Current issues and future directions of oncolytic adenoviruses. *Mol Ther* 2010; **18**: 243-250.
4 Clayman GL, el-Naggar AK, Lippman SM, Henderson YC, Frederick M, Merritt JA *et al.* Adenovirus-mediated p53 gene transfer in patients with advanced recurrent head and neck squamous cell carcinoma. *J Clin Oncol* 1998; **16**: 2221-2232.
5 Swisher SG, Roth JA, Nemunaitis J, Lawrence DD, Kemp BL, Carrasco CH *et al.* Adenovirus-mediated p53 gene transfer in advanced non-small-cell lung cancer. *J Natl Cancer Inst* 1999; **91**: 763-771.
6 Shimada H, Matsubara H, Shiratori T, Shimizu T, Miyazaki S, Okazumi S *et al.* Phase I/II adenoviral p53 gene therapy for chemoradiation resistant advanced esophageal squamous cell carcinoma. *Cancer Sci* 2006; **97**: 554-561.
7 Fujiwara T, Tanaka N, Kanazawa S, Ohtani S, Saijo Y, Nukiwa T *et al.* Multicenter phase I study of repeated intratumoral delivery of adenoviral p53 in patients with advanced non-small-cell lung cancer. *J Clin Oncol* 2006; **24**: 1689-1699.
8 Fujiwara T, Urata Y, Tanaka N. Telomerase-specific oncolytic virotherapy for human cancer with the hTERT promoter. *Curr Cancer Drug Targets* 2007; **7**: 191-201.
9 Pesonen S, Kangasniemi L, Hemminki A. Oncolytic adenoviruses for the treatment of human cancer: focus on translational and clinical data. *Mol Pharm* 2011; **8**: 12-28.
10 Bergelson JM, Cunningham JA, Droguett G, Kurt-Jones EA, Krithivas A, Hong JS *et al.* Isolation of a common receptor for Coxsackie B viruses and adenoviruses 2 and 5. *Science* 1997; **275**: 1320-1323.
11 Hemmi S, Geertsen R, Mezzacasa A, Peter I, Dummer R. The presence of human coxsackievirus and adenovirus receptor is associated with efficient adenovirus-mediated transgene expression in human melanoma cell cultures. *Hum Gene Ther* 1998; **9**: 2363-2373.
12 Hutchin ME, Pickles RJ, Yarbrough WG. Efficiency of adenovirus-mediated gene transfer to oropharyngeal epithelial cells correlates with cellular differentiation and human coxsackie and adenovirus receptor expression. *Hum Gene Ther* 2000; **11**: 2365-2375.
13 You Z, Fischer DC, Tong X, Hasenburg A, Aguilar-Cordova E, Kieback DG. Coxsackievirus-adenovirus receptor expression in ovarian cancer cell lines is associated with increased adenovirus transduction efficiency and transgene expression. *Cancer Gene Ther* 2001; **8**: 168-175.
14 Rauen KA, Sudilovsky D, Le JL, Chew KL, Hann B, Weinberg V *et al.* Expression of the coxsackie adenovirus receptor in normal prostate and in primary and metastatic prostate carcinoma: potential relevance to gene therapy. *Cancer Res* 2002; **62**: 3812-3818.
15 Kim M, Zinn KR, Barnett BG, Sumerel LA, Krasnykh V, Curiel DT *et al.* The therapeutic efficacy of adenoviral vectors for cancer gene therapy is limited by a low level of primary adenovirus receptors on tumour cells. *Eur J Cancer* 2002; **38**: 1917-1926.
16 Qin M, Chen S, Yu T, Escuadro B, Sharma S, Batra RK. Coxsackievirus adenovirus receptor expression predicts the efficiency of adenoviral gene transfer into non-small cell lung cancer xenografts. *Clin Cancer Res* 2003; **9**: 4992-4999.
17 Douglas JT, Kim M, Sumerel LA, Carey DE, Curiel DT. Efficient oncolysis by a replicating adenovirus (ad) *in vivo* is critically dependent on tumor expression of primary ad receptors. *Cancer Res* 2001; **61**: 813-817.
18 Fuxe J, Liu L, Malin S, Philipson L, Collins VP, Pettersson RF. Expression of the coxsackie and adenovirus receptor in human astrocytic tumors and xenografts. *Int J Cancer* 2003; **103**: 723-729.
19 Marsee DK, Vadysirisack DD, Morrison CD, Prasad ML, Eng C, Duh QY *et al.* Variable expression of coxsackie-adenovirus receptor in thyroid tumors: implications for adenoviral gene therapy. *Thyroid* 2005; **15**: 977-987.
20 Anders M, Rosch T, Kuster K, Becker I, Hofler H, Stein HJ *et al.* Expression and function of the coxsackie and adenovirus receptor in Barrett's esophagus and associated neoplasia. *Cancer Gene Ther* 2009; **16**: 508-515.
21 Korn WM, Macal M, Christian C, Lacher MD, McMillan A, Rauen KA *et al.* Expression of the coxsackievirus- and adenovirus receptor in gastrointestinal cancer correlates with tumor differentiation. *Cancer Gene Ther* 2006; **13**: 792-797.
22 Gu W, Ogose A, Kawashima H, Ito M, Ito T, Matsuba A *et al.* High-level expression of the coxsackievirus and adenovirus receptor messenger RNA in osteosarcoma, Ewing's sarcoma, and benign neurogenic tumors among musculoskeletal tumors. *Clin Cancer Res* 2004; **10**: 3831-3838.
23 Kawashima H, Ogose A, Yoshizawa T, Kuwano R, Hotta Y, Hotta T *et al.* Expression of the coxsackievirus and adenovirus receptor in musculoskeletal tumors and mesenchymal tissues: efficacy of adenoviral gene therapy for osteosarcoma. *Cancer Sci* 2003; **94**: 70-75.
24 Rice AM, Currier MA, Adams LC, Bharatan NS, Collins MH, Snyder JD *et al.* Ewing sarcoma family of tumors express adenovirus receptors and are susceptible to adenovirus-mediated oncolysis. *J Pediatr Hematol Oncol* 2002; **24**: 527-533.
25 Matsumoto K, Shariat SF, Ayala GE, Rauen KA, Lerner SP. Loss of coxsackie and adenovirus receptor expression is associated with features of aggressive bladder cancer. *Urology* 2005; **66**: 441-446.
26 Anders M, Vieth M, Rocken C, Ebert M, Pross M, Gretschel S *et al.* Loss of the coxsackie and adenovirus receptor contributes to gastric cancer progression. *Br J Cancer* 2009; **100**: 352-359.
27 Yamamoto S, Yoshida Y, Aoyagi M, Ohno K, Hirakawa K, Hamada H. Reduced transduction efficiency of adenoviral vectors expressing human p53 gene by repeated transduction into glioma cells *in vitro*. *Clin Cancer Res* 2002; **8**: 913-921.
28 Tango Y, Taki M, Shirakiya Y, Ohtani S, Tokunaga N, Tsunemitsu Y *et al.* Late resistance to adenoviral p53-mediated apoptosis caused by decreased expression of Coxsackie-adenovirus receptors in human lung cancer cells. *Cancer Sci* 2004; **95**: 459-463.
29 Sasaki T, Tazawa H, Hasei J, Kunisada T, Yoshida A, Hashimoto Y *et al.* Preclinical evaluation of telomerase-specific oncolytic virotherapy for human bone and soft tissue sarcomas. *Clin Cancer Res* 2011; **17**: 1828-1838.
30 Kawashima T, Kagawa S, Kobayashi N, Shirakiya Y, Umeoka T, Teraishi F *et al.* Telomerase-specific replication-selective virotherapy for human cancer. *Clin Cancer Res* 2004; **10** (1 Pt 1): 285-292.
31 Hashimoto Y, Watanabe Y, Shirakiya Y, Uno F, Kagawa S, Kawamura H *et al.* Establishment of biological and pharmacokinetic assays of telomerase-specific replication-selective adenovirus. *Cancer Sci* 2008; **99**: 385-390.
32 Kishimoto H, Kojima T, Watanabe Y, Kagawa S, Fujiwara T, Uno F *et al. In vivo* imaging of lymph node metastasis with telomerase-specific replication-selective adenovirus. *Nat Med* 2006; **12**: 1213-1219.
33 Kishimoto H, Urata Y, Tanaka N, Fujiwara T, Hoffman RM. Selective metastatic tumor labeling with green fluorescent protein and killing by systemic administration of telomerase-dependent adenoviruses. *Mol Cancer Ther* 2009; **8**: 3001-3008.
34 Kojima T, Hashimoto Y, Watanabe Y, Kagawa S, Uno F, Kuroda S *et al.* A simple biological imaging system for detecting viable human circulating tumor cells. *J Clin Invest* 2009; **119**: 3172-3181.
35 Kishimoto H, Zhao M, Hayashi K, Urata Y, Tanaka N, Fujiwara T *et al. In vivo* internal tumor illumination by telomerase-dependent adenoviral GFP for precise surgical navigation. *Proc Natl Acad Sci USA* 2009; **106**: 14514-14517.
36 Feero WG, Rosenblatt JD, Huard J, Watkins SC, Epperly M, Clemens PR *et al.* Viral gene delivery to skeletal muscle: insights on maturation-dependent loss of fiber infectivity for adenovirus and herpes simplex type 1 viral vectors. *Hum Gene Ther* 1997; **8**: 371-380.
37 Hoffman RM. The multiple uses of fluorescent proteins to visualize cancer *in vivo*. *Nat Rev Cancer* 2005; **5**: 796-806.
38 Hoffman RM, Yang M. Subcellular imaging in the live mouse. *Nat Protoc* 2006; **1**: 775-782.
39 Shay JW, Bacchetti S. A survey of telomerase activity in human cancer. *Eur J Cancer* 1997; **33**: 787-791.
40 Marsman WA, Buskens CJ, Wesseling JG, Offerhaus GJ, Bergman JJ, Tytgat GN *et al.* Gene therapy for esophageal carcinoma: the use of an explant model to test adenoviral vectors *ex vivo*. *Cancer Gene Ther* 2004; **11**: 289-296.
41 Wang Y, Thorne S, Hannock J, Francis J, Au T, Reid T *et al.* A novel assay to assess primary human cancer infectibility by replication-selective oncolytic adenoviruses. *Clin Cancer Res* 2005; **11**: 351-360.
42 Zeimet AG, Muller-Holzner E, Schuler A, Hartung G, Berger J, Hermann M *et al.* Determination of molecules regulating gene delivery using adenoviral vectors in ovarian carcinomas. *Gene Therapy* 2002; **9**: 1093-1100.
43 Kuster K, Koschel A, Rohwer N, Fischer A, Wiedenmann B, Anders M. Downregulation of the coxsackie and adenovirus receptor in cancer cells by hypoxia depends on HIF-1alpha. *Cancer Gene Ther* 2010; **17**: 141-146.

44 Seidman MA, Hogan SM, Wendland RL, Worgall S, Crystal RG, Leopold PL. Variation in adenovirus receptor expression and adenovirus vector-mediated transgene expression at defined stages of the cell cycle. *Mol Ther* 2001; **4**: 13-21.
45 Hotta T, Motoyama T, Watanabe H. Three human osteosarcoma cell lines exhibiting different phenotypic expressions. *Acta Pathol Jpn* 1992; **42**: 595-603.
46 Kawashima H, Ogose A, Gu W, Nishio J, Kudo N, Kondo N *et al.* Establishment and characterization of a novel myxofibrosarcoma cell line. *Cancer Genet Cytogenet* 2005; **161**: 28-35.
47 Kunisada T, Miyazaki M, Mihara K, Gao C, Kawai A, Inoue H *et al.* A new human chondrosarcoma cell line (OUMS-27) that maintains chondrocytic differentiation. *Int J Cancer* 1998; **77**: 854-859.

Supplementary Information accompanies the paper on Gene Therapy website (http://www.nature.com/gt)

European Journal of Cancer (2012) xxx, xxx–xxx

Available at www.sciencedirect.com

SciVerse ScienceDirect

journal homepage: www.ejconline.com

# A novel apoptotic mechanism of genetically engineered adenovirus-mediated tumour-specific p53 overexpression through E1A-dependent p21 and MDM2 suppression

Yasumoto Yamasaki [a], Hiroshi Tazawa [a,b], Yuuri Hashimoto [a], Toru Kojima [a], Shinji Kuroda [a], Shuya Yano [a], Ryosuke Yoshida [a], Futoshi Uno [a], Hiroyuki Mizuguchi [c], Akira Ohtsuru [d], Yasuo Urata [e], Shunsuke Kagawa [a], Toshiyoshi Fujiwara [a,*]

[a] *Department of Gastroenterological Surgery, Okayama University Graduate School of Medicine, Dentistry and Pharmaceutical Sciences, Okayama 700-8558, Japan*
[b] *Center for Gene and Cell Therapy, Okayama University Hospital, Okayama 700-8558, Japan*
[c] *Department of Biochemistry and Molecular Biology, Graduate School of Pharmaceutical Sciences, Osaka University, Osaka 565-0871, Japan*
[d] *Takashi Nagai Memorial International Hibakusha Medical Center, Nagasaki University Hospital, Nagasaki 852-8501, Japan*
[e] *Oncolys BioPharma Inc., Tokyo 105-0001, Japan*

**KEYWORDS**
Oncolytic adenovirus
Telomerase
p53
Apoptosis
p21

**Abstract** Oncolytic viruses engineered to replicate in tumour cells but not in normal cells could be used as tumour-specific vectors carrying the therapeutic genes. We previously developed a telomerase-specific oncolytic adenovirus, OBP-301, that causes cell death in human cancer cells with telomerase activities. Here, we further modified OBP-301 to express the wild-type *p53* tumour suppressor gene (OBP-702), and investigated whether OBP-702 induces stronger antitumour activity than OBP-301. The antitumour effect of OBP-702 was compared to that of OBP-301 on OBP-301-sensitive (H358 and H460) and OBP-301-resistant (T.Tn and HSC4) human cancer cells. OBP-702 suppressed the viability of both OBP-301-sensitive and OBP-301-resistant cancer cells more efficiently than OBP-301. OBP-702 caused increased apoptosis compared to OBP-301 or a replication-deficient adenovirus expressing the *p53* gene (Ad-p53) in H358 and T.Tn cells. Adenovirus E1A-mediated p21 and MDM2 downregulation was involved in the apoptosis caused by OBP-702. Moreover, OBP-702 significantly suppressed tumour growth in subcutaneous tumour xenograft models compared to monotherapy with OBP-301 or Ad-p53. Our data demonstrated that OBP-702 infection expressed adenovirus E1A and then inhibited p21 and MDM2 expression, which in turn efficiently induced apoptotic cell death. This novel apoptotic mechanism suggests that the p53-expressing OBP-702 is a promising antitumour reagent for human cancer and could improve the clinical outcome.


* *Corresponding author:* Address: Department of Gastroenterological Surgery, Okayama University Graduate School of Medicine, Dentistry and Pharmaceutical Sciences, 2-5-1 Shikata-cho, Kita-ku, Okayama 700-8558, Japan. Tel.: +81 86 235 7257; fax: +81 86 221 8775.
*E-mail address:* toshi_f@md.okayama-u.ac.jp (T. Fujiwara).

0959-8049/$ - see front matter © 2011 Elsevier Ltd. All rights reserved.
doi:10.1016/j.ejca.2011.12.020

Please cite this article in press as: Yamasaki Y. et al., A novel apoptotic mechanism of genetically engineered adenovirus-mediated tumour-specific p53 overexpression through E1A-dependent p21 and MDM2 suppression, *Eur J Cancer* (2012), doi:10.1016/j.ejca.2011.12.020

## 1. Introduction

Replication-selective oncolytic viruses have emerged as promising antitumour reagents for induction of tumour-specific cell death.[1–4] Recent evidence from several clinical studies of oncolytic virotherapy has suggested that oncolytic viruses are well tolerated by cancer patients.[5–8] We previously developed a telomerase-specific replication-competent oncolytic adenovirus OBP-301 (Telomelysin), in which the human telomerase reverse transcriptase (*hTERT*) promoter drives the expression of the *E1A* and *E1B* genes that are linked to an internal ribosome entry site (IRES).[9–11] A phase I clinical trial of OBP-301 in patients with advanced solid tumours has been recently completed and OBP-301 was well tolerated by these patients.[12] However, the antitumour effect of OBP-301 was limited in some of the OBP-301-injected tumours. Therefore, to efficiently eliminate tumour cells using OBP-301, and to improve the clinical outcome of cancer patients, enhancement of the OBP-301-mediated antitumour effect is required.

Genetically engineered armed oncolytic viruses that express several types of therapeutic transgenes have recently been reported that were aimed at enhancing the antitumour effect of an oncolytic virus.[6,13] Among candidate therapeutic transgenes, the tumour-suppressor *p53* gene is a potent therapeutic transgene for induction of cell cycle arrest, senescence and apoptosis.[14] Indeed, a p53-expressing replication-deficient adenovirus (Ad-p53, Advexin) has been reported to induce an antitumour effect in both *in vitro* and *in vivo* settings[15,16] as well as in various clinical studies.[17–20] Recently, p53-expressing armed replication-selective oncolytic adenoviruses have been shown to induce a stronger antitumour effect than a non-armed oncolytic adenovirus or Ad-p53.[21–23] However, the molecular mechanism of the enhanced antitumour effect of a p53-armed oncolytic adenovirus remains unclear. We recently showed that, in combination therapy, OBP-301 enhanced Ad-p53-mediated apoptosis through p53 upregulation and by suppression of the p53-downstream target p21,[24] which is not only transcriptionally activated and mainly induces cell cycle arrest, but also suppresses apoptosis.[25] These results suggest that this p53-expressing oncolytic adenovirus has a strong antitumour effect through apoptosis induction.

In the present study, we first investigated whether the p53-expressing telomerase-specific replication-competent oncolytic adenovirus OBP-702 has efficient *in vitro* antitumour activity compared with OBP-301. We next compared the induction of apoptotic cell death of human cancer cells infected with OBP-301, OBP-702 and Ad-p53. The molecular mechanism of OBP-702-mediated apoptosis induction was further addressed. Finally, the *in vivo* antitumour effect of OBP-702 was evaluated using two subcutaneous human tumour xenograft models.

## 2. Materials and methods

### 2.1. Cell lines

The human non-small cell lung cancer cell lines H1299 (p53 null), H358 (p53 null) and H460 (wild-type p53) were obtained from the American Type Culture Collection (Manassas, VA, USA). The human oesophageal cancer cell line T.Tn (mutant-type p53) was purchased from the Japanese Collection Research Bioresources (JCRB, Osaka, Japan). The human oral squamous cell carcinoma cell line HSC4 (wild-type p53) was obtained from the Human Science Research Resources Bank (HSRRB, Osaka, Japan). The human colon cancer cell lines (SW620 (mutant-type p53) and LoVo (wild-type p53)) and the human liver cancer cell line HepG2 (wild-type p53) were obtained from the American Type Culture Collection (Manassas, VA, USA). The human liver cancer cell line Huh-7 (mutant-type p53) was obtained from the Human Science Research Resources Bank (HSRRB, Osaka, Japan). H1299, H358, H460, T.Tn, SW620 and LoVo cells were maintained in RPMI 1640 medium. HSC4, HepG2 and Huh-7 cells were maintained in Dulbecco's modified Eagle's medium. All media were supplemented with 10% foetal bovine serum, 100 U/ml penicillin and 100 mg/ml streptomycin. The cells were routinely maintained at 37 °C in a humidified atmosphere containing 5% $CO_2$.

### 2.2. Recombinant adenoviruses

The recombinant telomerase-specific, replication-competent adenovirus OBP-301 (Telomelysin), in which the promoter element of the *hTERT* gene drives the expression of *E1A* and *E1B* genes that are linked with an IRES, was previously constructed and characterised.[9–11] For OBP-301 induction of exogenous *p53* gene expression, a human wild-type *p53* gene expression cassette derived by the Egr-1 promoter was inserted into the E3 region of OBP-301 (Fig. 1A). The E1A-deleted adenoviral vector dl312 and the wild-type adenovirus type 5 (Ad5) were used as control vectors. Recombinant viruses were purified by ultracentrifugation using caesium chloride step gradients, their titres were determined by a plaque-forming assay using 293 cells, and viruses were stored at −80 °C.

### 2.3. Western blot analysis

Cells were seeded in a 100-mm dish at a density of $1 \times 10^5$ cells/dish 12 h before infection and were infected with OBP-301, OBP-702 or Ad-p53 at the indicated multiplicity of infection (MOI). Whole cell lysates were prepared in a lysis buffer (50 mM Tris–HCl (pH 7.4), 150 mM NaCl, 1% Triton X-100) containing a protease inhibitor cocktail (Complete Mini; Roche, Indianapolis,

Please cite this article in press as: Yamasaki Y. et al., A novel apoptotic mechanism of genetically engineered adenovirus-mediated tumour-specific p53 overexpression through E1A-dependent p21 and MDM2 suppression, *Eur J Cancer* (2012), doi:10.1016/j.ejca.2011.12.020